The International Workshop of Technology of Earthquake Monitoring and Geophysical data Analysis Application

&

The 16th Japan-Taiwan International Workshop on Hydrological and Geochemical Research for Earthquake Prediction

Program and Abstracts

September 5-6, 2017

International Conference Hall, Central Weather Bureau

Contents

Venue Map

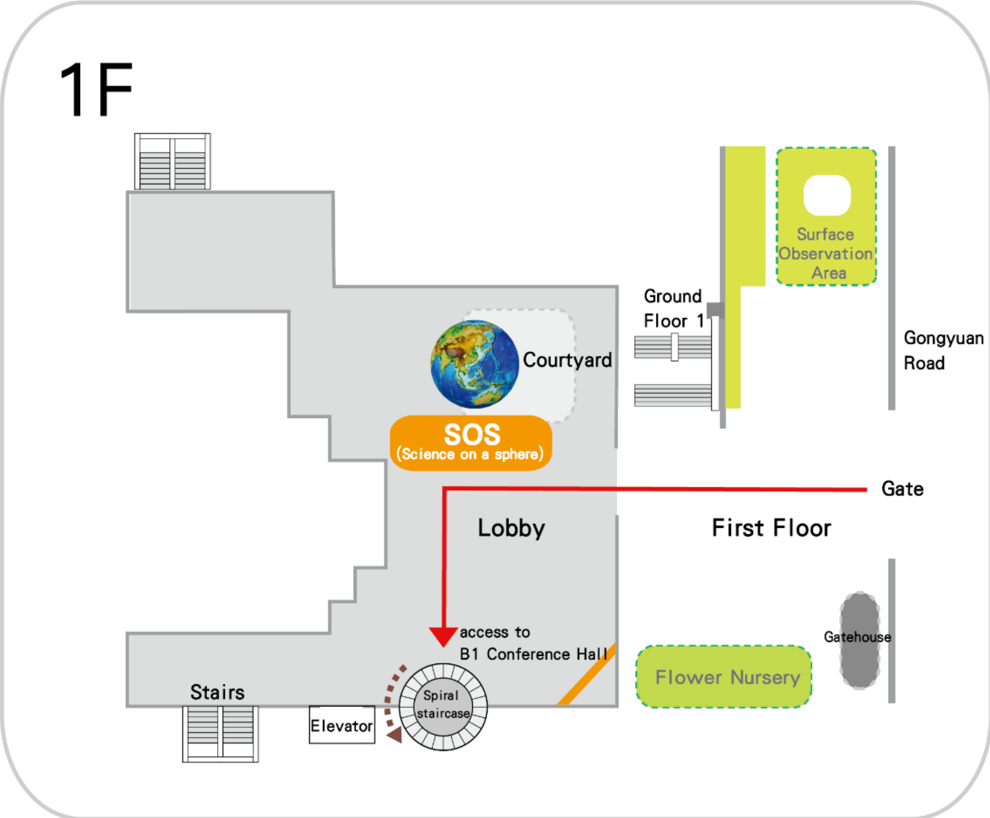
1F
Courtyard
SOS
(Science on a sphere)
Ground
Floor 1
Surface
Observation
Area
Gongyuan
Road
Gate
Lobby
First Floor
access to
B1 Conference Hall
Gatehouse
Flower Nursery
Stairs
Elevator
Spiral
staircase

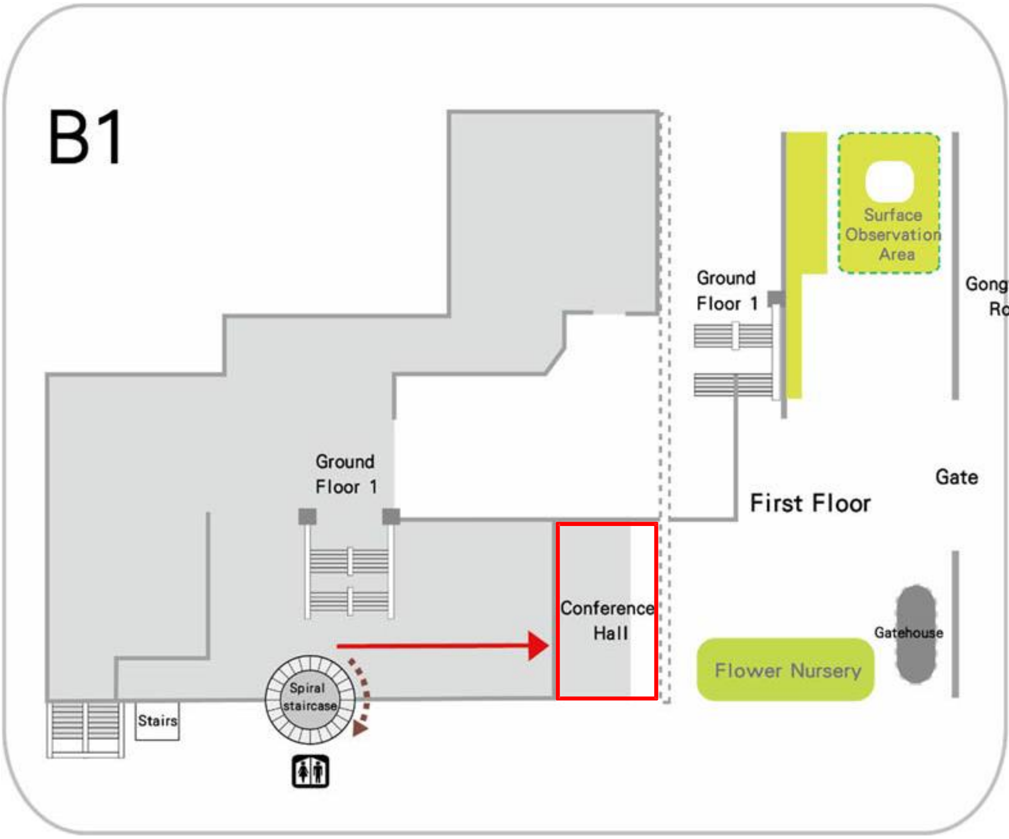
B1
Ground
Floor 1
Surface
Observation
Area
Gongyuan
Road
Ground
Floor 1
Gate
First Floor
Conference
Hall
Gatehouse
Flower Nursery
Spiral
staircase
Stairs

Agenda Sep. 5 (Tue)

TIME	VENUE	PROGRAM
08:00~08:40	Reception	Registration
08:40~09:00	Conference Hall	Opening Ceremony
		Opening Remarks & Group Photo

Session-1 (*host: Kuo-Fong Ma & Yoshiyuki Kaneda*)			
TIME	**SPEAKER**	**TOPIC**	**PAGE**
09:00~09:20	Masataka Ando	Is southern Ryukyu subduction zone is seismically decupled? A speculation based on onshore and offshore geodetic data	5
09:20~09:40	Shu-Kun Hsu	Seismic clustering in the western end of the Ryukyu subduction zone	7
09:40~10:00	Ryoya Ikuta	Back-arc opening in the western end of the Okinawa trough revealed by GNSS/Acoustic Ocean-floor geodesy off Ilan, Taiwan	9
10:00~10:20	Yoshiyuki Kaneda	Ocean floor network systems and advanced simulation researches in Japan	13
10:20~10:40	Ban-Yuan Kuo	Deep sea circulation determined from OBS tilt noise	17

10:40~11:00	**BREAK & POSTER SESSION**

Agenda Sep. 5 (Tue)

TIME	PROGRAM		
Session-2 *(host: Masataka Ando & Shu-Kun Hsu)*			
TIME	**SPEAKER**	**TOPIC**	**PAGE**
11:00~11:20	Kuo-Fong Ma	Fault zone physical property examination through borehole seismometers	19
11:20~11:40	Norio Matsumoto	Detection of short-term slow slip events by groundwater pressure sealed by borehole packer in a deep well	21
11:40~12:00	Ya-Ju Hsu	Hydrological effects to borehole strainmeters in eastern Taiwan	25
12:00~12:20	Kuo-Liang Wen	Microearthquake monitoring for the Sanchiao Fault	27

12:20~13:00	**LUNCH & POSTER SESSION**

TIME	PROGRAM		
Session-3 *(host: Chung-Pai Chang & Ryoya Ikuta)*			
TIME	**SPEAKER**	**TOPIC**	**PAGE**
13:00~13:20	Yuzo Ishikawa	Redetermination of several hypocenters of the Utsu catalog in Taiwan area (1906-1925)	29
13:20~13:40	Bor-Shouh Huang	Re-examination of the 1990 Ms=7.8 Luzon Earthquake Sequence Based On Seismic Observations Recorded By A Dense Regional Seismic Network In Taiwan	33
13:40~14:00	Chung-Pai Chang	Structural Study of the Earthquake Source Areas in Taiwan	35
14:00~14:20	Wen-Tzong Liang	Regional and Global W-Phase Source Inversion Systems developed in Taiwan	37
14:20~14:40	Shiann-Jong Lee	Toward the Real-time Computational Seismology Earthquake Report in Taiwan	39
14:40~15:00	Po-Fei Chen	High resolution 3-D velocity structures of NE Taiwan and its tectonic implications	41

15:00~15:20	**BREAK & POSTER SESSION**

Agenda Sep. 5 (Tue)

TIME	PROGRAM		
Session-4 *(host: Naoji Koizumi &* Jann-Yenq Liu *)*			
TIME	**SPEAKER**	**TOPIC**	**PAGE**
15:20~15:40	Jann-Yenq Liu	Characteristics of pre-earthquake ionospheric anomalies of the total election content	43
15:40~16:00	Chien-Chih Chen	Testing the correlations between anomalies of statistical indexes of the geoelectric system and earthquakes	45
16:00~16:20	Fumiaki Tsunomori	Groundwater monitoring for geochemical studies on earthquake related phenomena	47
16:20~16:40	Ching-Chou Fu	Anomalous radon and gamma rays changes as a precursor of major earthquake in northern Taiwan	49
16:40~17:00	Kuniyo Kawabata	Change of groundwater radon concentration caused by The 2016 Kumamoto earthquake	51
17:00~17:20	Min-Chien Tsai	Pre-seismic anomalous observations before large earthquake in Taiwan: Insight from CWB geophysical data	55
SESSION1~4 END			

Potential landslide tsunami risk in Taiwan

(Is southern Ryukyu subduction zone is seismically decupled? A speculation based on onshore and offshore geodetic data)

Masataka Ando[1*]

1. Center for Integrated Science and Education of Natural Hazards, Shizuoka University, 836 Oya, Suruga, Shizuoka,422-8529, Japan
(andomasataka@gmail.com)

It is estimated that around 7 % of tsunamis involve submarine landslides on Earth (Harbitz et al., 2014). Landslides are ubiquitous features of submarine slopes in all geological settings and at all water depths (Masson et al., 2006). Submarine gravity flow deposits can be used for finding large earthquakes in many places. For example, the analysis of slides and turbidites along the Oregon-Washington margin suggests that magnitude ~9 earthquakes occurred every 590 years on average (Adams, 1990); the turbidite stratigraphy in the Japan trench is similar to that of onshore tsunami deposits, indicating that at least three large earthquakes have occurred near the epicenter of the 2011 Tohoku-oki earthquake during the past 1,500 years (Ikehara et al., 2016).

Submarine landslides similarly often occur in Taiwan. Off the coast of Ilan, NE Taiwan, episodic turbidity deposits in the Okinawa trough are correlated in space and time to large (ML >6.8) submarine earthquakes since the 20th century (Huh et al., 2004). Submarine landslides and turbidity currents were triggered by the 2006 M7.0 Pingtung earthquakes offshore SW Taiwan, causing major failures in international telecommunication cables (Hsu et al., 2008). Non-seismic submarine landslides during the 2009 Morakot Typhoon were also found in broadband seismograms recorded in Taiwan and Japan (Lin et al., 2009). Sea waves caused by theses landslides were not observable in tide gauge records.

In the 19th century, there were two local tsunami-like waves may have struck the east coast of Taiwan. A large sea wave struck an area of Chenggong in the middle of the 19th century according to an oral history of the area (Ando et al., 2013). Another large wave may have struck an area of Fenbin between 1855 and 1878. The wave was inferred to be a tsunami instead of storm waves generated by a typhoon (Ando et al., 2015). Nevertheless, there is not definite evidence to verify that theses large waves were tsunamis. These events were not well noticed in the western half of the Taiwan and not have been recorded. One possible cause for each local large wave is a small submarine landslide off the coast of Chenggong or Fengbin. They may have been triggered by an earthquake or by gravitational instability.

Tectonically active plate margins are characterized by relatively small failures (< 2km^3) such as Mediterranean (McAdoo, 2004) and Cascadia subduction zone (Urgeles et al., 2013). The risk of large landslide tsunamis may be low in tectonically active Taiwan, but the risk of small landslide tsunamis may be potentially high. A more complete mapping of landslide sources would certainly improve assessment of landslide tsunami potential. For the past events, mechanical analyses of the release, disintegration, and flow mechanisms will help in understanding landslide dynamics. Furthermore, detailed bathymetric surveys are necessary to resolve this issue.

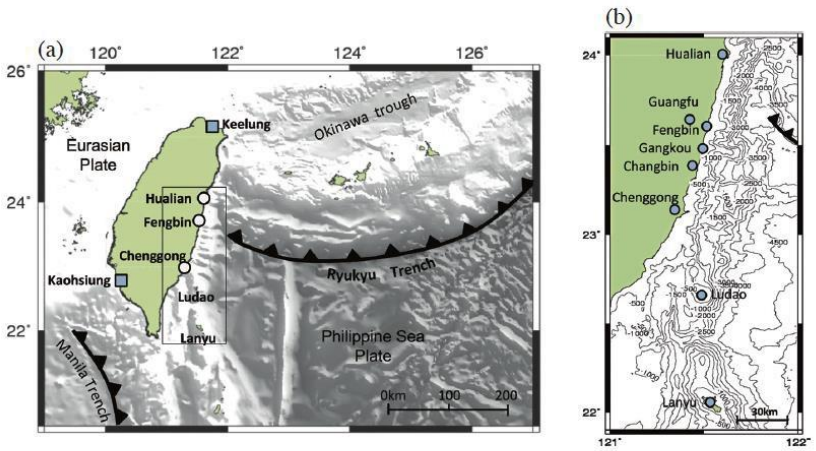

Fig. 1. (a) Map showing the bathymetry around Taiwan. The rectangle depicts the survey area of this study. It also shows Keelung and Koushing, where the 1867 tsunami and 1781 tsunami were observed, respectively, according to historical documents. (b) Locality map of the interview sitesof this study. (After Ando et al., 2015)

NOTES

Seismic clustering in the western end of the Ryukyu subduction zone

Shu-Kun Hsu[1,*], Shiou-Ya Wang[1] and Yi-Ching Yeh[1]

1. Department of Earth Sciences, National Central University, Taiwan
(hsu@ncu.edu.tw)

The border between two colliding plates usually involves a complex crustal deformation and generates abundant earthquakes along the convergent boundary. Due to the strong collision, the contiguous zone of the two plates may create a shear zone to accommodate the plate motion, such as the Ailao Shan-Red River shear zone in the India-Eurasia collision or the North Anatolia Fault shear zone in the Anatolia-Eurasia collision. In the case of the active Taiwan orogen between the Philippine Sea Plate and Eurasian Plate, the collision in northeast Taiwan is progressively evolving into the subduction along the west Ryukyu Trench. In consequence, the Taiwan-Ryukyu junction area consists of more than 70% earthquakes around Taiwan island. Particularly, an intensively seismic clustering occurs along the subducting plate interface off eastern Taiwan, which includes several large earthquakes and the largest earthquake of magnitude 8 ever recorded in Taiwan. However, the mechanism of the seismic clustering was poorly understood. Here we demonstrate a shear zone acts as the transform boundary in the junction area. We adope a model of restraining strain due to a step-over in the sheared zone to account for the seismic clustering phenomenon beneath the Hoping Rise and Nanao Basin. The localized and enhanced stress probably has triggered large earthquakes in the complex border between two colliding plates.

Keywords: Ryukyu Trench, seismic cluster, sheared zone

NOTES

Deformation of the Ryukyu arc and north-eastern Taiwan Island at the western end of the Okinawa trough based on GNSS/Acoustic seafloor geodesy

(Back-arc opening in the western end of the Okinawa trough revealed by GNSS/Acoustic Ocean-floor geodesy off Ilan, Taiwan)

Horng-Yue Chen[1], Ryoya Ikuta[2,3*], Ya-Ju Hsu[1], Takeru Kohmi[3], Cheng-Horng Lin[1], Yoko Tu[4], Chau-Chang Wang[5], Shui-Bei Yu[2] and Masataka Ando[2]

1. Institute of Earth Science, Academia Sinica
2. Center for Integrated Science and Education of Natural Hazards, Shizuoka University
3. Graduate School of Integrated Science and Technology, Shizuoka University
4. Department of Natural History Sciences, Faculty of Science, Hokkaido University
5. Institute of Undersea Technology National Sun Yat-Sen University

We measured seafloor movement using GNSS/Acoustic technique at the south of the rift valley in western end of the Okinawa trough back-arc basin. The seafloor site was installed at the halfway between Taiwan and Yonaguni Islands in July 2012.

The horizontal position of the benchmark, measured eight times during the period from July 2012 to May 2016, showed southward movement suggesting back-arc opening of the Okinawa trough. The average velocity of the OILN site shows block motion together with Yonaguni Island. This block at western most end of the Ryukyu arc rotates clockwise. The easting velocity of OILN is higher than those of sites on Taiwan Island which suggests that the OILN is not pushed by but pulled apart from the Taiwan Island. This rotation of OILN should cause the expansion of Ilan plain and northern part of the Central Mountain Range of Taiwan observed by GNSS data [Hou et al.2009].

Introducing this new block to the end of the Okinawa arc, we re-examined two block boundary models of the Ryukyu arc defined by previous works (Nakamura [2004]; Nishimura et al. [2004]) introducing the Yonaguni block. Based on AIC, the boundary model in which Yaeyama and Miyako islands are on different blocks which expand in along-trench direction (Nakamura [2004]) is regarded as a better model. However, among the rigid block models, a model with the boundary at Kerama gap east to Miyako Island (Nishimura et al. [2004]) is regarded to be better. However, among the rigid

block models, boundary at the Kerama gap at the east of Miyako Island was better (Nishimura et al. [2004]).

Considering the transient motion of the seafloor benchmark with seismicity, not abrupt but gentle episodic opening of the rifting valley accompanying a moderate seismic activation is suggested.

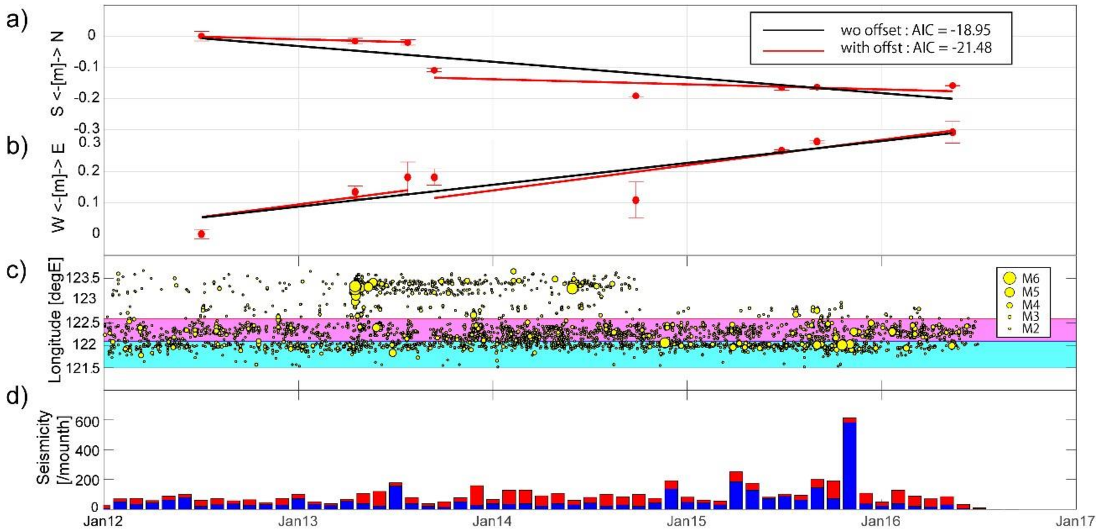

Figure 1. Time series of OILN site with reference to stable part of Yangtze plate. (a) North-South and (b) East-West displacement of the benchmark. Red and black lines are fitting lines with and without an offset, respectively. (c) Epicenters of earthquakes detected during the period within the rectangular shown in the Figure 2. The areas hatched by red and blue represent the ranges from 122.1 to 122.5°E and from 121.5 to 122.1°E, respectively. (d) Monthly seismicity within the area hatched by magenta and cyan in (c) are shown as red and blue bars, respectively.

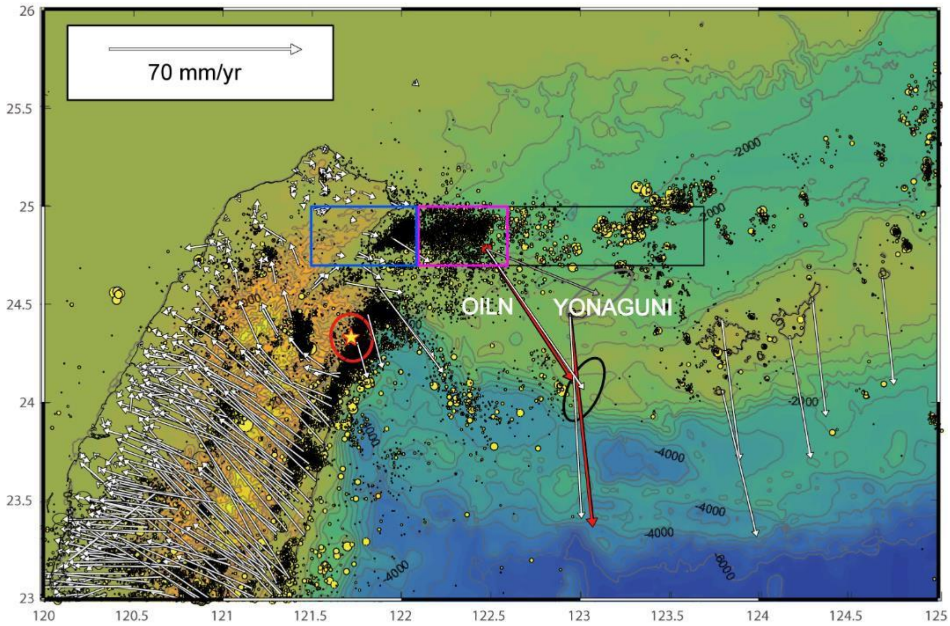

Figure 2 Observed velocity vectors (white arrows) in our OILN GNSS/Acoustic site, YONAGUNI GEONET, and other GNSS sites. The red arrows show the predicted velocity vector as Yonaguni rigid block. The star shows the Euler pole of Yonaguni block. The error ellipses show the 95% confidence intervals. Circles show the epicenter of earthquakes shallower than 20km.

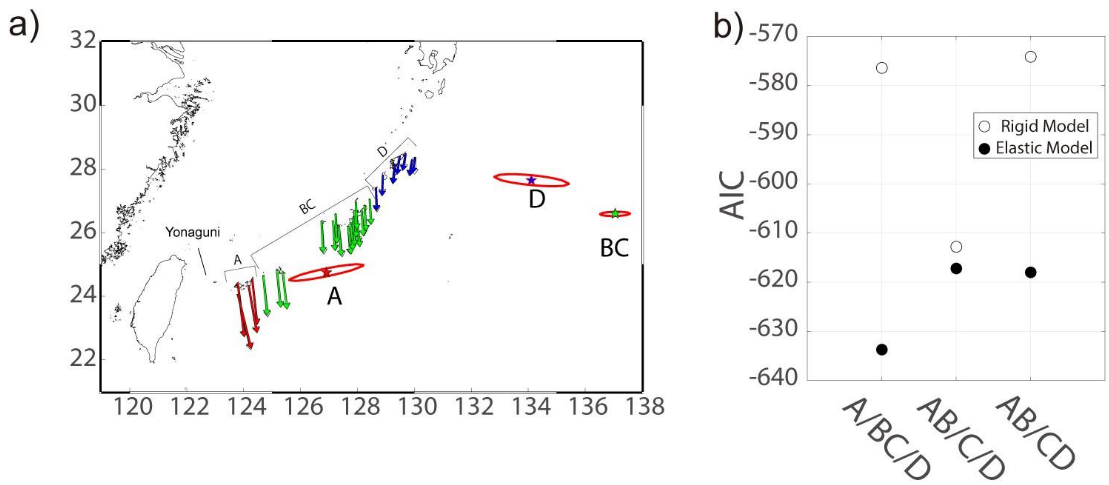

Figure 3. (a) The optimal block model. Observed velocity vectors are shown by open arrows. Colored arrows show the velocity vectors predicted by the best 1-D expanding block model. (b) Calculated AIC values with block boundary models assumed in this study. Open and black circles correspond to rigid block and 1-D expanding models, respectively.

Acknowledgements

We acknowledge Central Weather Bureau in Taiwan for providing hypocenter of the earthquakes. Geospatial Information Authority of Japan and the Japan Meteorological Agency provided the coordinate of GEONET and seismicity data in Japan, respectively. This study was supported by a grant (NSC 101-2116-M-001-025) from the National Science Council of Taiwan.

NOTES

Ocean floor network systems and advanced simulation researches in Japan

Yoshiyuki Kaneda[1,2,,3*]
and
Narumi Takahashi[2,3], Ksuyoshi Kawaguchi[2], Takane Hori[2], Eiichiro Araki[2],, Hiroyuki Matsumoto[2], Takeshi Nakamura[3], Shinichiro Kamiya[2], Keisuke Ariyoshi[2], Mamoru Hyodo[2], Masaru Nakano[2], Jin-Kyu choi[2], Shuhei Nishida[2], Takashi Yokobiki[2]

1. Kagawa University
2. Japan Agency for Marine-Earth Science and Technology (JAMSTEC)
3. National Research Institute for Earth Science and Disaster Resilience (NIED)

In this paper, attention has been particularly drawn to destructive Earthquakes and Tsunamis, such as 1999 Chichi Earthquake in Taiwan, 1999 Izumit Earthquake in Turkey, 2004 Sumatra Earthquake/Tsunami in Indonesia, 2008 Wenchuan Earthquake in China, 2010 Chile Earthquake/Tsunami, and 2011 East Japan Earthquake/Tsunami.

Based on lessons learned from 2011 East Japan Earthquake and Tsunami, we recognized the importance of real time monitoring of these natural hazards. Therefore, as real time monitoring system, DONET1 (Dense Ocean floor Network for Earthquakes and Tsunamis) was deployed and DONET2 is being developed around the Nankai trough southwestern Japan. Furthermore, DONET1 and DONET2 (Fig.1) with multi kinds of sensors such as broadband seismometers and precise pressure gauges will be expected to monitor slow events such as low frequency tremors and slow earthquakes for the estimation of seismic stage which is the inter-seismic or pre-seismic stage based on slow event simulation researches. Not only slow events, but also the change of micro seismicity will be significant for the estimation of seismic stage (Fig.2).

Furthermore, advanced simulations such as the recurrence cycle of mega thrust earthquakes, tsunami inundation and seismic response on buildings /city are very important for future disaster mitigation programs and related measures. Now, we are developing to the Tsunami estimation system with the integration of real time monitoring data and tsunami simulation database. If this system is practical, it is very powerful for the estimation of damages by tsunamis and evacuation and rescue.

In 2016 April 1st earthquake of M6.5 occurred off Kii Peninsula, this earthquake' hypocenter is located beneath DONET1 array around the Tonankai Earthquake seismogenic zone southwestern Japan after 70 years from 1944 Tonankai Earthquake (Fig.3). Therefore, we can analyzed this earthquake in detail. Based on analyses of this earthquake, we simulated the transition of seismicity.

According to the recurrence cycle simulation, if the earthquake of over M6.3 occur, this earthquake can trigger thenext Tonankai earthquake. So, the real time monitoring and simulation researches are indispensable for not only the advanced early warning system but also the understanding of transition on crustal activities after earthquakes.

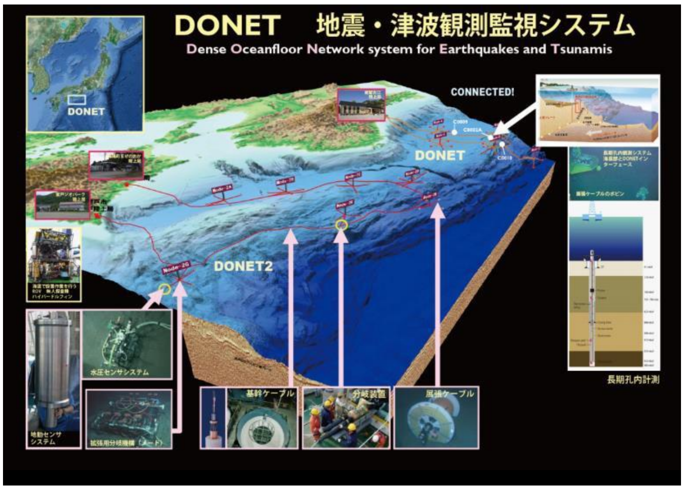

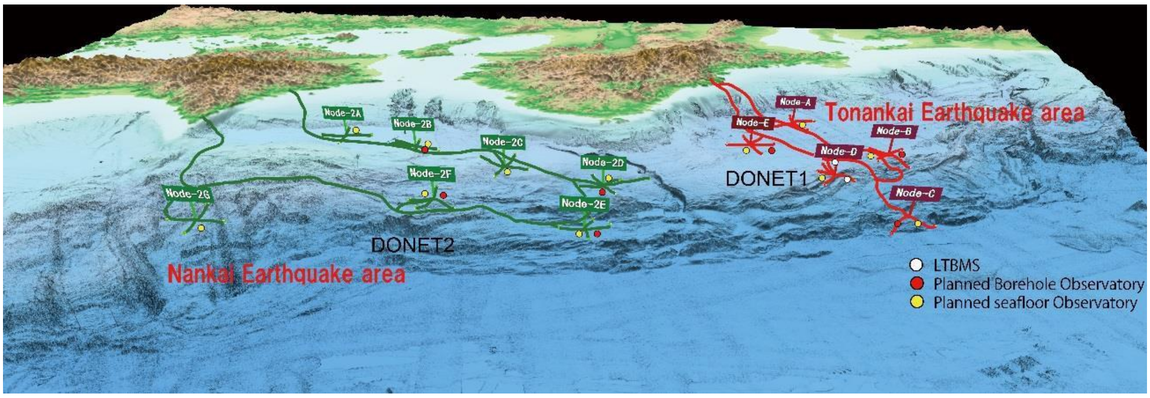

Fig 1: The outline of DONET1 and DONET2 arrays.　　JAMSTEC
DONET1 has been deployed off Tonankai earthquake seismogenic zone

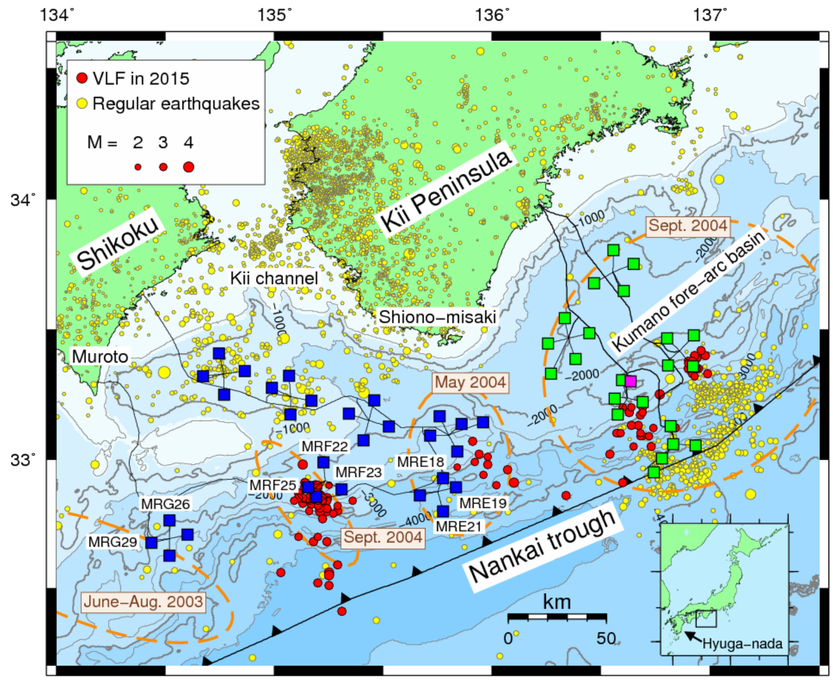

Nakano et al. (2016 EOS)

Fig.2.: Map showing the DONET stations (green squares, DONET1; blue squares, DONET2) and the borehole station (purple square in the DONET1 network area) along the Nankai trough and the fiber-optic cables (black lines) connecting them.

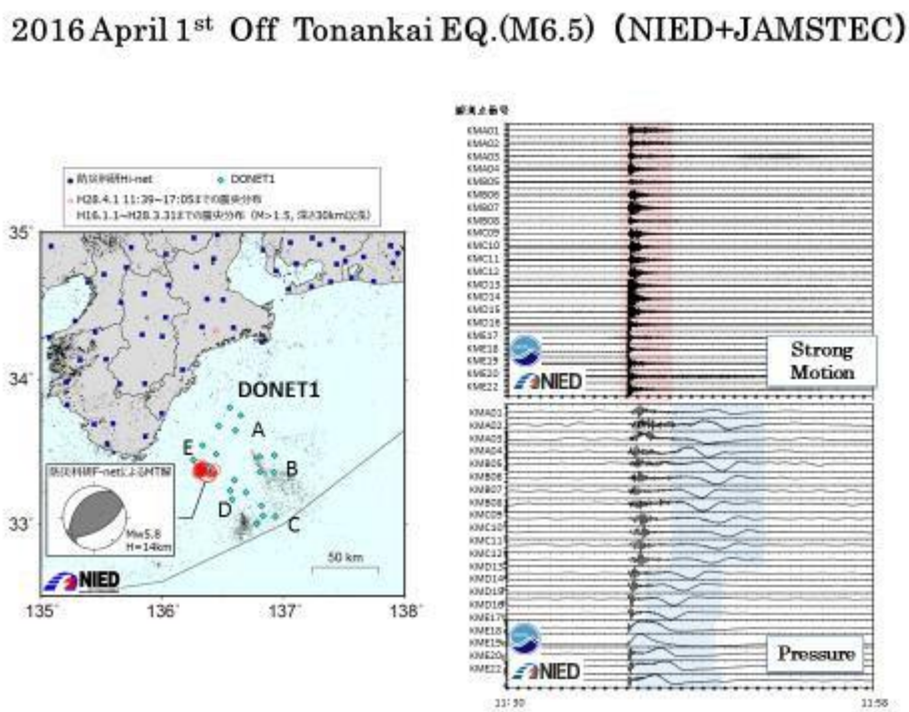

Fig.3: The 2016 April 1st Earthquake of M6.5 recorded by DONET1

NOTES

Deep sea circulation determined from OBS tilt noise

Ban-Yuan Kuo[1*], Pei-Ying Patty Lin[2], Jian-Ming Liau[2], and Ching-Ren Lin[1]

1. Institute of Earth Sciences, Academia Sinica, Taipei, Taiwan
2. Taiwan Ocean Research Institute, National Applied Research Labs, Kaohsiung

(byk@earth.sinica.edu.tw)

Ocean-bottom seismometer (OBS) records both seismic waves and ocean waves. The former are received as the sensor shakes in response to the ground motion caused by an earthquake. The latter are registered in the motion of the sensor pushed by ocean waves. The ocean wave signals, or noise as we usually see them from a seismological viewpoint, are embedded in the OBS data. Tilt noise dominates the horizontal component when bottom current rocks the sensor housing out of its balanced position because the sensor housing is not fixed on the seafloor. We found long period tilt noise in the OBS data deployed in the Okinawa trough and the open Pacific ocean that are related with the semidiurnal tides. The relationship between horizontal and vertical tilt lends a possibility to constrain the directivity of the bottom current, and the Okinawa trough data offer an opportunity to test against the local ocean wave model. The directivity of the tidal waves can be simulated by taking into account all modes of tides and seafloor topography confirms a westward motion of the tidal wave The tilt data shows the presence of bottom circulation westward at each OBS site. The results suggest a scenario in which the westward bottom current, probably driven by tides, pushes the OBS sensor housing to tilt one-sided towards the west without being pushed back as the wave returns elsewhere. However, in very few exception cases that the OBS tilt noise does not behave in accordance with this scenario. We are in the process of verification of the tide-tilt noise relationships and planning an installation of ocean-bottom current meter as the in-situ measurement.

Keywords: OBS, tilt noise, ocean wave

NOTES

Fault Zone Physical Properties Investigation From Borehole Seismometers

Kuo-Fong Ma[1*], and EPSL members[2]
1. Institute of Geophysics, National Central University, Taoyuan, Taiwan
2. EPSL, Earthquake Physics and Seismotectonic Laboratory, National Central University

We investigated fault zone physical properties on attenuation, anisotropy, stress status through Taiwan Chelungpu-fault Drilling Project Borehole Seismometers (TCDPBHS), and CWB new generation borehole seismic array. TCDPBHS were installed through the identified fault zone (~950m-1300m) to monitor the micro-seismic activities after a large earthquake, as well as the fault-zone seismic structure properties. CWB borehole ranged from the depth of 100m-350m over the islandof Taiwan. The attenuation structure was examined through spectra ratio of surface and borehole arrays for CWB borehole stations, and stations above and below fault zone for TCDPBHS. It shows low Qp and Qs in the fault zone as down to about 30 within fault zone, and good correlation of shallow Qp and Qs structure with heat flow distribution. The fault zone anisotropy and the stress status were carried out by physical logs and borehole seismometer cross-correlation analysis. We analyzed cross-correlation of the noise at different stations to obtain cross correlation functions (CCFs) between each station pairs. The result shows that TCDP well site suffers from complex wavefield, and phase traveltime from CCF can't provide explicit result to determine the dominated wavefield. We also analyze the Fourier spectral amplitudes by rotating every 5 degrees in time domain to search for the maximum background energy distribution. The result shows that the spectral amplitudes are stronger at NE-SW direction, with shallow incident angles which is comparable with the CCF particle motion measurement. In order to obtain higher resolution about the dominated wavefield in our study area, we also used beamforming from surface station array to validate our results from CCF analysis. In addition to the CCF analysis to provide the noise configuration at the TCDPBHS site for further analysis on fault zone anisotropy using ambient noise. We also analyze fault zone anisotropy using the events data recorded by TCDPBHS. The identified event clusters through the borehole data enhance the consistency in results to give hints on fault zone anisotropy. It shows the rotation of the stress status over the fault zone as indicated from the maximum fastest axis in anisotropy. The rotation of the stress axis is consistent with physical logging analysis through FMI. Further study on the temporal

variation of the stress status over the fault is intriguing in understanding fault zone healing process from stress recovering prospective.

NOTES

Detection of changes in aquifer pressure associated with short-term slow slip events in a deep well sealed by borehole packer

Yuichi Kitagawa and Norio Matsumoto*
(Geological Survey of Japan, AIST)

In terms of fault-model estimation of short-term slow slip events (S-SSEs) occurring at the plate boundary of the Nankai Trough, one of the issues to be solved is that there are no observation sites of crustal deformation with a high quality in the western part of Aichi prefecture and the northern part of Mie prefecture. In this area, there is HKS observation well (Fig.1), but unfortunately, the well water level had a small response to tidal strain (0.05 mm/nstrain in M_2 constituent), because the aquifer in this well has a low permeability and the diameter of the well is large.

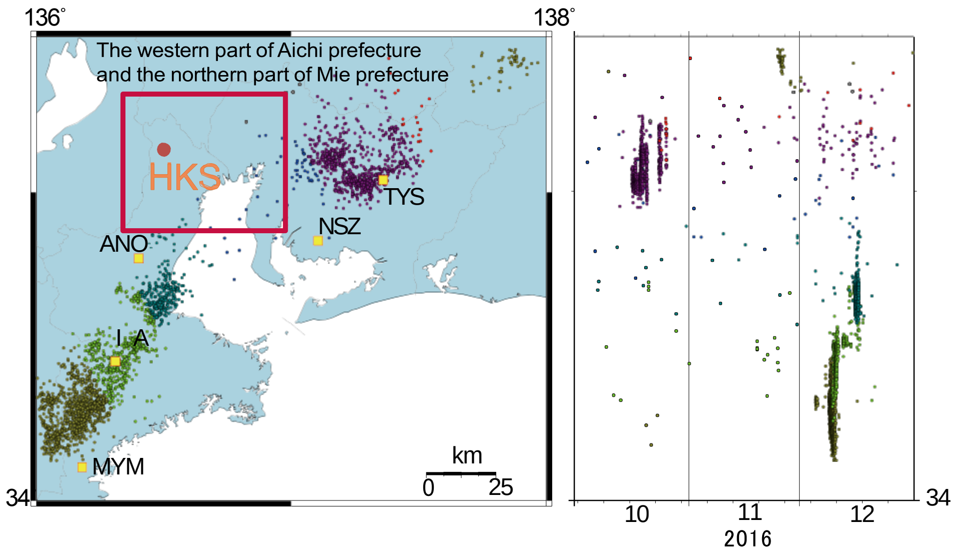

Fig.1 Location of HKS observation site and space-time distribution of deep low frequency tremors from Oct. 2016 to Dec. 2016.

The sensitivity of the aquifer pressure to crustal deformation depends only on the mechanical properties of the aquifer (e.g. shear modulus, undrained Poisson's ratio and Skempton's coefficient; Roeloffs, 1996). Meanwhile, the sensitivity of the well water level to crustal deformation depends not only on the sensitivity of the aquifer pressure, but also on permeability of the aquifer and the diameter of the well because a finite time is required for flow into and out of the well to equilibrate the well water level and aquifer pressure. This phenomenon is referred to as 'wellbore storage effect'. If the diameter of the well is large, and/or the aquifer permeability is low, the well water level is not able to track the aquifer pressure, and the sensitivity of well water level to crustal deformation is significantly attenuated (Hsieh et al.,1987; Matsumoto and Roeloffs, 2003).

Our objective is to directly observe the aquifer pressure at the HKS observation well in order to obtain information of the crustal deformation with high sensitivity. We deployed a borehole packer to seal the casing pipe of the HKS observation well and started to observe aquifer pressure at the well.

After the sealing the well, the response of the aquifer pressure to tidal strain is 0.498 mm/nstrain in M_2 constituent, and is improved about 10 times than the response of well water level to tidal strain before the sealing the well (Fig.2). By eliminating the tidal, barometric-pressure and rainfall responses from the observed aquifer pressure, the changes in the residual aquifer pressure associated with S-SSEs around the Ise Bay are detected in July and December 2016. We compare the detected changes in aquifer pressure with calculated changes from the fault models of the S-SSEs determined by borehole strainmeters and tiltmeters.

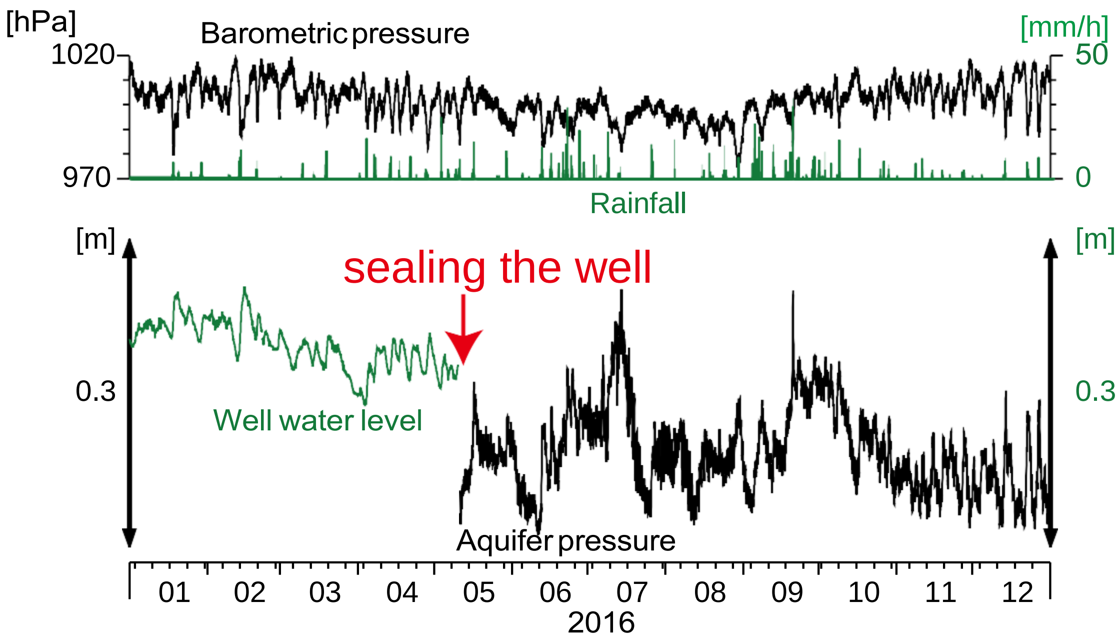

Fig.2 Well water level before sealing the well, aquifer pressure after sealing the well, barometric pressure and rainfall at HKS observation site.

References

Hsieh, P.A., Bredehoeft, J.D. and Farr, J.M., 1987. Determination of aquifer transmissivity from Earth tide analysis, *Water Resour. Res.*, **23,** 1824–1832.

Matsumoto, N. and Roeloffs, E.A., 2003. Hydrological response to earthquakes in the Haibara well, central Japan: II. Possible mechanism inferred from time-varying hydraulic properties, *Geophys. J. Int.*, **155,** 899-913.

Roeloffs, E.A., 1996. Poroelastic techniques in the study of earthquake related hydrologic phenomena, in *Advances in Geophysics*, Vol. 37, pp. 135–195, ed. Dmowska, R., Academic, San Diego.

NOTES

Hydrological effects to borehole strainmeters in eastern Taiwan

Ya-Ju Hsu[1*]

1. Institute of Earth Sciences, Academia Sinica, Taipei, Taiwan
(yaru@earth.sinica.edu.tw)

Taiwan experiences high deformation rates, particularly along its eastern margin where a shortening rate of about 30 mm/yr is experienced in the Longitudinal Valley and the Coastal Range. Four Sacks-Evertson borehole strainmeters have been installed in this area since 2003. *Liu et al*. (Nature, 2009) proposed that a number of strain transient events, primarily coincident with low barometric pressure during passages of typhoons, were due to deep triggered slow slip. Here we extend that investigation with a quantitative analysis of the strain responses to precipitation as well as barometric pressure and the earth tides in order to isolate tectonic source effects. Estimates of the strain responses to barometric pressure and ground water level changes for the different stations vary over the ranges -1~-3 nanostrain/millibar(hPa) and -0.3~-1.0 nanostrain/hPa, respectively, consistent with theoretical values derived using Hooke's law. *Liu et al*. (Nature, 2009) noted that during some typhoons, including at least one with very heavy rainfall, the observed strain changes were consistent with only barometric forcing. By considering a more extensive data set we now find the strain response to rainfall is about -5.1 nanostrain/hPa. A larger strain response to rainfall compared to that to air pressure and water level may be associated with an additional strain from fluid pressure changes that take place due to infiltration of precipitation. Using a state-space model, we remove the strain response to rainfall, in addition to those due to air pressure changes and the earth tides and investigate whether corrected strain changes are related to environmental disturbances or tectonic-original motions. The majority of strain changes attributed to slow earthquakes seem rather to be associated with environmental factors. However some events show remaining strain changes after all corrections. Additional on-site water level sensors and rain gauges will provide data critical for a more complete understanding including the currently unresolved issue of why, for some typhoons, there appears to be a much smaller transfer function for precipitation induced strain changes.

Keywords: Borehole strainmeter, precipitation, typhoons, slow slip

NOTES

Microearthquake monitoring for the Sanchiao Fault

Kuo-Liang Wen [1*], Che-Min Lin [2], Chih-Wei Chang [3]

1. Department of Earth Sciences, National Central University, Taiwan. (wenkl@cc.ncu.edu.tw)
2. National Center for Research on Earthquake Engineering, NARlabs, Taiwan. (cmlin@narlabs.org.tw)
3. National Center for Research on Earthquake Engineering, NARlabs, Taiwan. (chihwei@ncree.narl.org.tw)

The Shanchiao fault is the major active fault in northern Taiwan. The normal faulting caused the Taipei Basin and is the largest potential seismic threat to the Taipei metropolitan area. Furthermore, there is a dormant volcano, the Tatun volcano, located at the southwestern hanging wall of the Shanchiao fault. The complex tectonic environment makes the seismicity of this fault unclear. In this study, a real-time microearthquake monitoring network was set up with thirteen broadband seismometers to observe the seismicity of the Shanchiao fault continuously since April 2015. Additional thirty-five stations operated by the other three organizations are integrated with our monitoring. The integrated monitoring data provide valuable information about recent seismicity and the source parameters, which are indispensable in assessing the seismic potential of the Shanchiao fault.

Almost 2000 microearthquakes were located in the monitoring region until now. Most of the epicenters concentrate on the Tatun volcano area. The focal depths are mostly within 5 km. The double-difference earthquake location algorithm (HypoDD) was used to relocate the earthquakes observed by the network, and the focal mechanisms for some events were computed from P-wave first motion polarities. According to these results, several earthquake clusters happened in this region were identified. Although the involving of the Tatun volcano make it hard to clarify the seismicity of the Shanchiao fault, we hope that the probable seismogenic structures and source ruptures can be evaluated by long-term monitoring in the future.

Keywords: earthquake monitoring, Shanchiao fault, earthquake location, focal mechanism.

NOTES

Redetermination of several hypocenters of the Utsu catalog in Taiwan area (1906-1925)

Yuzo Ishikawa[1*]

1. Research Institute of Earthquake and Volcano Geology, Geological Survey of Japan, AIST

Japan Meteorological Agency(JMA) redetermined hypocenters using old seismological bulletins from 1923 to 1960. These bulletins reported P and S wave arrival times of many stations including seismic stations in Taiwan. These hypocenters in and around Taiwan are shown in Fig.1a and Fig.1b. Most of hypocenters in JMA earthquake catalog in Taiwan were from 1922 to 1942. And several not all hypocenters in 1943 and 1944 were reported.

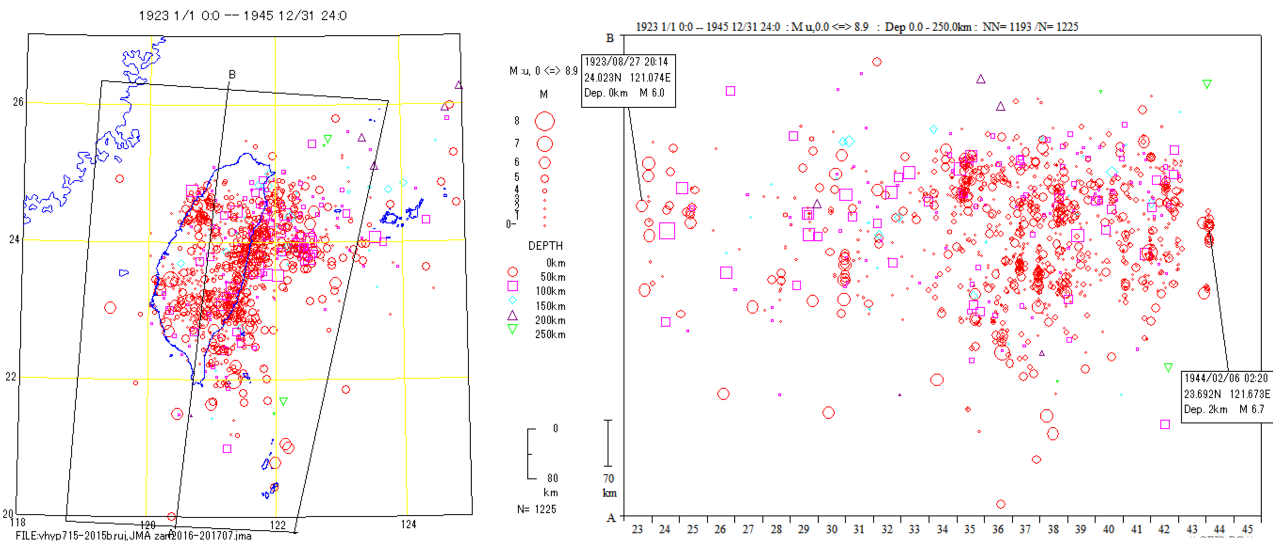

Figure 1a (Left): Hypocenter distribution by JMA earthquake catalog in and around Taiwan from 1923 to 1945. Figure 1b (Right): Time-space distribution of hypocenters in the cut down area in figure 1a. It is clear that a part of earthquakes were determined hypocenters after 1943 and no hypocenters after 1945.

Before 1923, the Utsu catalog and the ISC-GEM catalog were openly used for reseach. The Utsu catalog included 25 events and ISC-GEM catalog 16 events from 1900 to 1923 in and around Taiwan. The hypocenters of ISC-GEM catalog were determined by ISC, but ones of the Utsu catalog were only listed in the paper by Utsu. Generally, it is rather hard to determine hypocenters in early 20 century, as seismic stations were sparse and the clocks at the seismic stations were not so accurate.

Here, for avoiding the uncertainty of P and S arrival times, the differences of P and S arrival times at each seismic stations were used to estimate hypocenters. Travel time table JMA2001 (Ueno et.al, 2001) which was routinely used by JMA was adopted for stations of which epicentral distance were less than 2000km and Jeffreys & Bullen's table for more than 2000km. The locations of ols seismic stations were also checked, as some present seismic stations were located at the different places from old seismic stations. The locations of old seismic stations were observed by GPS, referring Hong(2007).

Several new hypocenters were obtained by this way. Two samples were shown in Figure 2 and 3.

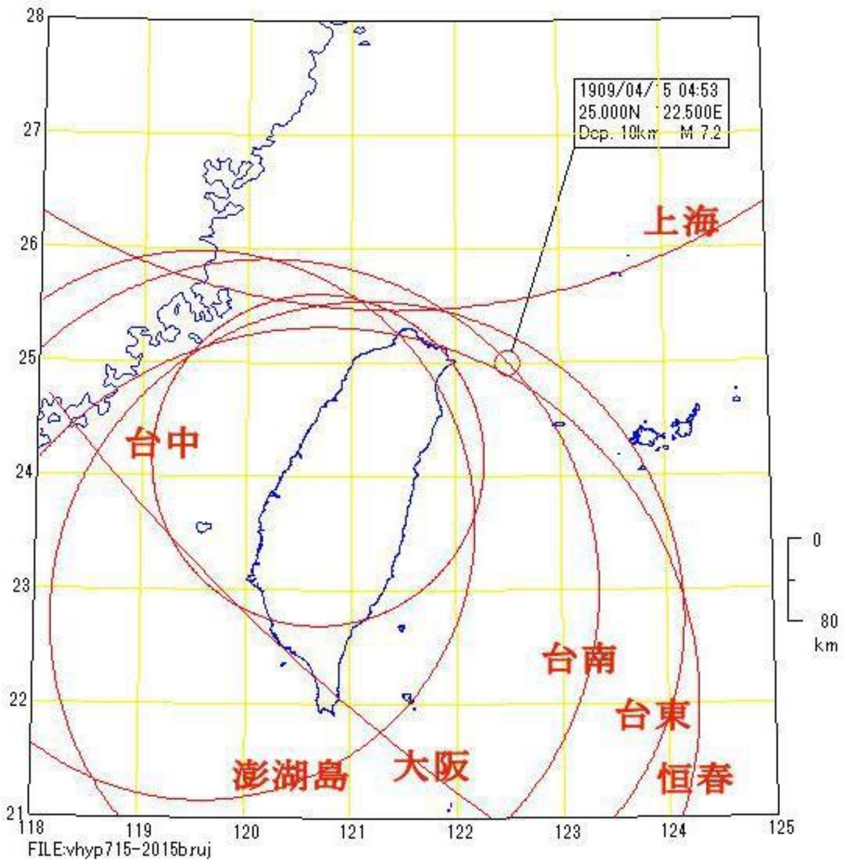

Figure 2: The hypocenter of 1909 April 14 19:53(UT) M7.3 earthquake was estimated by S-P times of 7 seismic stations. The hypocenter depth was assumed as 80 km to draw circles. Open circle shows the hypocenter of the Utsu catalog.

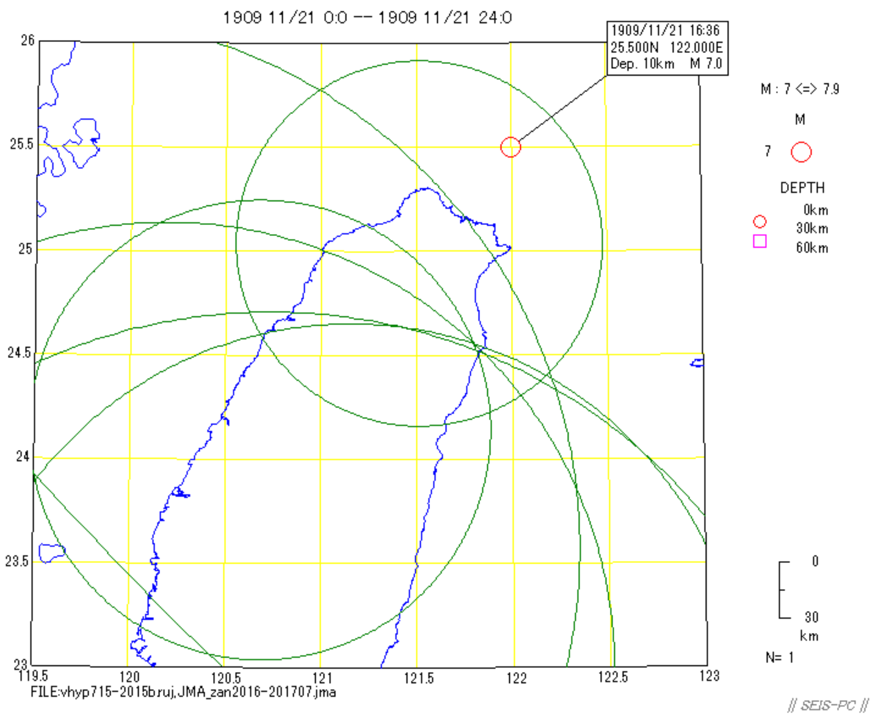

Figure 3: The hypocenter of 1909 Nov. 11 07:36(UT) M7.0 earthquake was estimated by S-P times of 7 seismic stations. The hypocenter depth was assumed as 10km to draw circles. Open circle shows the hypocenter of the Utsu catalog.

Reference

Hong Chih-wen,2007，台湾気象伝奇，玉山社,293pp.

JMA travel time tables;

http://www.data.jma.go.jp/svd/eqev/data/bulletin/catalog/appendix/trtime/trt_j.html#ttt

NOTES

Re-examination of the 1990 M_s=7.8 Luzon earthquake sequence based on seismic observations recorded by a dense regional seismic network in Taiwan

Bor-Shouh Huang[1], Win-Gee Huang[1], Po-Fei Chen[2], Ishmael Narag[3], Bartolome C. Bautista[3] and Renato U. Solidum Jr.[3]

1. Institute of Earth Sciences, Academia Sinica, Nankang, Taipei, Taiwan
2. Department of Earth Sciences, National Central University, Tayuon, Taiwan
3. Department of Science and Technology, Philippine Institute of Volcanology and Seismology, Quezon City, Philippines

The Luzon earthquake with a 7.8 M_s magnitude occurred on July 16, 1990 in the Philippines. The earthquake produced a 125 km-long ground rupture along the Philippine Fault System. This event is one of largest strike-slip earthquakes ever recorded in the world and its aftershock area extended more than 100 km along the fault zone from the north to its southern end. The source rupture process and its aftershocks distribution have been detailed studied using the global seismic network observations and its crustal deformation from a regional GPS network. However, limited regional and local observations and analysis were reported.

Actually, within a thousand kilometer distance of this earthquake epicenter, there was a dense seismic network named the Taiwan Telemetered Seismographic Network (TTSN) installed and continuous operation (since 1972) to monitor earthquakes occurring in Taiwan and its surrounding area. During this earthquake, 24 stations of this network were well operated to record the main shock and its aftershock. Each station equipped either 1-Hz 3-component seismometer, or 1-Hz vertical-component seismometer, transmitted its seismic signals through telephone line to its recording center. The signals are made digitally at 100 samples/sec at the recording center. Timing is provided by a crystal-controlled time-of-day clock, which keeps time to which a few milliseconds a day to the standard time.

In this study, after 25 years of earthquake occurrence, we plan to relocate aftershocks of this earthquake and its source detail using modern analyzed seismological techniques developed in recent years. Thus, based on relative location of main shock, those aftershocks will be relocated and test for source imaging of this earthquake using array observed high-frequency seismograms of the TTSN.

NOTES

Structural Study of the Earthquake Source Areas in Taiwan

Chung-Pai Chang [1, 2*], Yi-Chun, Hsu [2]

1. Center for Space and Remote Sensing Research, National Central University, Jhongli, 32001 Taoyuan
2. Institute of Geophysics, National Central University, Jhongli, 32001 Taoyuan

(cpchang@csrsr.ncu.edu.tw)

Taiwan is located on an active orogenic belt where the Philippine Sea plate converges toward the Eurasian plate with a speed of 8.2 cm per year. This rapid convergence induced dramatic crustal deformation, very active faults and high seismic activities in Taiwan, and brought numerous earthquake disasters. In order to assess the potential earthquake disasters, the local geological survey is crucial. Moreover, for conducting the post-seismic planning and for reducing the following damage, the earthquake geological research of the near-epicenter area right after the large earthquake is also essential. In This study we select some high earthquake potential areas on the basis of previous studies to carry out a series of detail geological surveys. In case of large earthquake happens, we first use the satellite images to illustrate the co-seismic surface deformation, and conduct the geological survey over the near-epicenter area immediately afterward the earthquake. We will demonstrate some cases in the past few years to show the importance of geological survey for earthquake study.

Keywords：geological survey, earthquake potential, co-seismic surface deformation.

NOTES

Regional and Global W-Phase Source Inversion Systems developed in Taiwan

Wen-Tzong Liang[1*] Wen-Hui Lee[1] Chin-Shang Ku[2]

1. Institute of Earth Sciences, Academia Sinica, Taiwan. (wtl@earth.sinica.edu.tw; hui@earth.sinica.edu.tw)
2. Department of Geoscience, National Taiwan University (backnew@earth.sinica.edu.tw)

It has been proven that the W-Phase (WP) source inversion can offer a reliable moment magnitude for strong earthquake in a short time, which may in turn provide valuable information for seismic hazard assessment. This algorithm has been widely used at various data centers in the world. In this study, we have developed both regional and global scales of real-time automated WP source inversion systems to identify the earthquake rupture process and a more robust moment magnitude (Mw) for moderate to strong earthquakes occurred in the Taiwan region. To achieve these goals, we firstly implement a SeisComP data acquisition system and take advantage of publicly shared real-time waveform data streams from various agencies to monitor global seismicity. Once the estimated magnitude for a detected event is larger than 6, then the Global WP (gWP) source inversion system will be triggered to start retrieving and processing available waveforms for inverting all the focal mechanism parameters, including Mw, strike, dip, slip, moment tensor, scalar moment, CLVD, and waveform fittings. On the other hand, the regional WP source (WP) inversion is triggered by the earthquake alert issued by Central Weather Bureau of Taiwan. Only regional exchanged waveforms are used to reduce the computing time. To give an appropriate estimate of half duration time, shift time and filtered frequency band, we take empirical Mw dependent constraints suggested by previous researchers. Furthermore, both the hypocenter and shift-time will be calibrated through a grid search approach around the initial guesses. This strategy enables these two systems to run automatically in a robust way. For the regional system, we are able to invert WP solution for event with magnitude as small as 4.5. To take the challenge of the determination of reliable Mw and rupture behavior for future strong earthquakes, these two systems may play an important role while the local waveforms were clipped or suffered from power outage. Please refer to online websites at http://tesis.earth.sinica.edu.tw, http://tecdc.earth.sinica.edu.tw/FM/gWP and http://tesis.earth.sinica.edu.tw/world/ for more information.

Keywords: Earthquake Focal Mechanism, W-Phase Source Inversion, CMT.

NOTES

Toward the Real-time Computational Seismology Earthquake Report in Taiwan

Shiann-Jong Lee[1*], Wen-Tzong Liang[1], Bor-Shouh Huang[1]

1. Institute of Earth Sciences, Academia Sinica, Taiwan
(sjlee@earth.sinica.edu.tw)

Real-time earthquake report based on computational seismology is currently possible to be achieved which needs highly connection between high quality seismic network and high performance computing. In the recent seismic monitoring systems, the information of an earthquake report are mostly based on observations. The precision of source parameters and shaking intensity distribution is restricted by both density and quality of a seismic network. In addition, further to obtain a focal mechanism always require some lag time before obtaining the rapid earthquake information. Here, we develop a Real-time Computational Seismology (RCS) earthquake report which contains a real-time moment tensor monitoring system and a real-time online earthquake simulation system. The Real-time Moment Tensor (RMT) monitoring system used high quality continuous broadband records and moment tensor inversion technique. The RMT provides all the source parameters, including the event origin time, hypocentral location, moment magnitude and full moment tensor, within 2 minutes after the occurrence of an earthquake. Then, these source parameters are automatically forwarded to the Real-time Online earthquake Simulation (ROS) system to perform an island-wide earthquake simulation based on 3D spectral-element method. The online simulation system provides ShakeMovie and ShakeMap automatically in less than 3 minutes. With these two parts together, an earthquake report based on computational seismology can be provided within 5 minutes after an earthquake occurs in Taiwan. The RCS earthquake report includes: (1) event occurrence time, (2) hypocenter location, (3) moment magnitude, (4) full moment tensor, (5) ShakeMovie, (6) ShakeMaps, (7) intensity map, (8) coseismic surface displacement, and (9) synthetic waveforms. This system is operated online at the Institute of Earth Sciences, Academia Sinica (*http://rcs.earth.sinica.edu.tw/*) since 2015. The long-term goal of RCS system is to provide a comprehensive rapid earthquake report for public based on computational seismology and to give contribution for seismic hazard assessment in real-time.

Keywords: real-time, computational seismology, earthquake report

NOTES

High Resolution 3-D Velocity Structures of NE Taiwan and Its Tectonic Implications

Po-Li SU[1#], Po-Fei CHEN[1], Hao KUO-CHEN[1], Chien-Ying WANG[1], Chien-Hsin CHANG[2], Wen-Tzong LIANG[3]

1. National Central University, Taiwan
2. Central Weather Bureau, Taiwan
3. Academia Sinica, Taiwan

#Corresponding author: polisu@g.ncu.edu.tw

The Ilan plain in NE Taiwan locates on the southwest end of the Okinawa trough, a back arc basin of the Ryukyu subduction, and abuts Central Range (CR) to the south and Hsuehshan Range (HR) to the northwest. Knowing crust and upper mantle structures beneath NE Taiwan is thus crucial to understanding the subduction-collision transition of the Eurasia–Philippine Sea plate boundaries. We aim at inverting high resolution 3-D velocity structures by deployinf a dense seismic network of Texan instrument in Ilan Plain, which consists of 109 vertical component sensors with ~2 km interval distance. On top of that, nearby stations of Central Weather Bureau Seismic Network and Japan Meteorological Agency, i.e., YOJ, are combined to relocate earthquakes used for inversion and to enlarge inversion area. Having employed finite difference tomography algorithm (Roecker et al., 2006) with checkerboard test, the resolutions can reach ~8km^3 at shallow (0~20km) and ~16km^3 at depth up to 80 km depth for targeting area. Results show low velocities just beneath Taipei basin and Ilan plain. While those beneath Taipei exhibit continuous feature of downward extension southeasterly to the low velocity zones of mantle wedge, those of beneath Ilan instead seem more connected to the low velocity zone of offshore back-arc basin. On the other hand, the high velocity zones exhibit clear slab features all the way beneath from offshore to Eastern Central Range above 40 km depth, corresponding Collision Seismic Zone induced by collision between PSP and EUP (Kao et al., 1998).

References

Kao, H., Shen, S. J., and Ma, K. F., 1998. Transition from oblique subduction to collision: Earthquakes in the southernmost Ryukyu arc-Taiwan region. Journal of Geophysical Research: Solid Earth, 103(B4), 7211-7229.

Roecker, S., Thurber, C., Roberts, K., and Powell, L., 2006. Refining the image of the San Andreas Fault near Parkfield, California using a finite difference travel time computation technique. Tectonophysics, 426(1), 189-205.

NOTES

Characteristics of pre-earthquake ionospheric anomalies of the total election content

Jann-Yenq (Tiger) Liu[1*]

1. Institute of Space Science, National Central University, TAIWAN

Ground-based observations of the GPS TEC (total electron content) and satellite probing of radio occultation (RO) of FORMOSAT-3/COSMIC (F3/C) are employed to study the co-seismic disturbances and precursors of the 11 March 2011 M9.0 Tohoku earthquake. It is for the first time the tsunami origin observed. The horizontal propagation of seismo-traveling ionospheric disturbances (STIDs) induced by tsunami and seismic waves of the Tohoku earthquake are observed by the GPS TEC, while the associated vertical propagation is probed by multi ground-based observations and F3/C RO sounding. The raytracing and beamforming techniques are used to find the propagation and origin of the STIDs triggered by the seismic and tsunami waves. Meanwhile, z test and the Receiver Operating Characteristic (ROC) curve are employed to find the characteristic of the temporal SIPs (seismo-ionospheric precursor) of the GIM (global ionosphere map) TEC associated with earthquakes in Japan during 1998-2014. It is found that anomalies appearing 3 days before the Tohoku earthquake well agree with the characteristic, which suggests that the SIPs of the earthquake have been observed. A global study on the distribution of anomalies shows that the SIPs specifically and continuously occur over the epicenter on 8 March 2011, 3 days prior to the Tohoku earthquake. Finally, a physical model of the ionosphere is used to reproduce the observed anomalies and find possible causal of the Tohoku SIPs.

NOTES

Testing the correlations between anomalies of geoelectric field statistics and earthquakes

Hong-Jia Chen[1*], Chien-Chih Chen[1]

1. Department of Earth Science, National Central University, Jhongli, Taiwan
(redhouse6341@gmail.com)

Although the feasibility of the earthquake precursor and prediction is still debated, a few scientists, such as Varotsos, Eftaxias, Uyeda, etc., reliably find that the geomagnetic and geoelectric anomalies precede large earthquakes. They analyze the geomagnetic and geoelectric signals based on statistical physics and critical transition. They think that earthquake rupture is a critical point, and the crustal system would approach this point during an earthquake preparation process. In critical transition theory, the dynamics of systems near a critical point have generic properties, such as increasing autocorrelations, flickering, changing skewness, etc. Hence, the geophysical measurement might present some of those properties during the earthquake preparation process. However, those previous studies are of case study. Therefore, we do not know whether the defined precursory indexes are correlated earthquakes. In this study, we test the forecasting skills and provide evidence of the precursory nature within systematic analyses on full time series. The data sets include Taiwan earthquake catalog and geoelectric fields with 1-Hz sampling rate. The research methods involve calculations of skewness and kurtosis on geoelectric fields, development of earthquake-forecasting algorithm, and evaluation of model performance by Molchan diagram. The major findings suggest that the anomalies of skewness and kurtosis of geoelectric fields are related to large earthquakes. The strategy of model selection to forecast earthquakes are also discussed. The results of this study may help to build up ensemble forecasting probability of earthquakes and to approach the earthquake forecasts.

Keywords: skewness, kurtosis, earthquake precursor, geoelectric field, Molchan diagram.

NOTES

Groundwater monitoring for geochemical studies on earthquake related phenomena

Fumiaki Tsunomori[1*]

1. Geochemical Research Center, Graduate School of Science, The University of Tokyo.

A continuous gas monitoring system was reconfigured. As reported in the 15th workshop last year, a ternary composition of helium, nitrogen and argon in dissolved gas in groundwater, which is sampled from an aquifer connected to the Atotsugawa fault, might have respond to crustal deformation around the Atotsugawa fault. Hence, we adjusted the monitoring system to be suitable to measure these three species. So far, dissolved gas was analyzed only in our old system, however atmospheric air is also measured in the new system automatically. In addition, we automatically evaluate abundances of crustal origin gas, mantle origin gas and air origin gas under a few assumptions every day. As fluctuation of trajectory of ternary composition of atmospheric air in a triangle plot is small, time variation of ternary composition of dissolved gas in groundwater is not artifact.

Conclusions

1. A continuous monitoring system of dissolved gas in groundwater was re-configured in order to focus time variation of ternary composition.

2. As fluctuation of trajectory of ternary composition of atmospheric air in a triangle plot is small, time variation of ternary composition of dissolved gas in groundwater is not artifact.

Corresponding Author Email address: eqpred@gmail.com (Fumiaki Tsunomori)

Preprint submitted to 16-th Japan-Taiwan International Workshop August 7, 2017

NOTES

Anomalous radon and gamma rays changes as a precursor of major earthquake in northern Taiwan

Ching-Chou Fu[1*], Lou-Chuang Lee[1], Tsanyao Frank Yang[2], Cheng-Horng Lin[1], Cheng-Hong Chen[2], Vivek Walia[3]

1. Institute of Earth Sciences, Academia Sinica, Taiwan
2. Department of Geosciences, National Taiwan University, Taiwan
3. National Center for Research on Earthquake Engineering, NARL, Taiwan

(ccfu@earth.sinica.edu.tw)

Taiwan is tectonically situated in a terrain resulting from the oblique collision between the Philippine Sea plate (PHS) and the Eurasian plate (EU). The continuous observations of soil radon for earthquake studies at the Tapingti station (TPT) have been recorded and are compared with the data from gamma rays observations at the Taiwan Volcano Observation station (YMSG), located north to the TPT station. Some anomalous high radon concentrations and gamma-ray counts at certain times can be identified. It is noted that the significant increase of soil radon concentrations were observed and followed by the increase in gamma-ray counts several days before the earthquakes, which occurred in northeastern Taiwan. These earthquakes are usually located within the subducting PHS beneath the EU to the north along the Ryukyu trench in northern Taiwan (e.g., M_L=6.3 April 20, 2015). It is suggested that the pre-seismic activities of an earthquake may be associated with slow geodynamic processes at the subduction interface, leading to the PHS movement to trigger radon enhancements at TPT station. Furthermore, the further movement of PHS may be locked by EU and accumulate elastic stress resulting in the increase of gamma rays due to an increase in the porosity and fractures below the YMSG station. The continuous monitoring on the multiple parameters can improve our understanding of the relationship between the observed radon and gamma-ray variations and the regional crustal stress/strain in the area.

Keywords: radon, gamma ray, earthquake, subduction

NOTES

Change of groundwater radon concentration caused by 2016 Kumamoto earthquake

Kuniyo Kawabata*[1,2], Takahiro Hosono[3], Tsutomu Sato[4], Hiroshi A. Takahashi[4], Kiyoshi Ide[3] and Yujin Kitamura[1]

1. Graduate School of Science and Engineering, Kagoshima University
2. JSPS research fellow
3. Faculty of Science, Kumamoto University
4. AIST, Geological Survey of Japan, Institute of Earthquake and Volcano Geology

The 2016 Kumamoto earthquake struck central Kumamoto prefecture on April 14 (Mw 6.2 foreshock) and 16 (Mw 7.0 main shock) and caused huge damage around the area. The area of a series of the events and the aftershocks, Beppu, Aso and Central Kumamoto prefecture, is situated along the active Beppu-Shimabara rift. It is explained that the main shock and foreshock ruptured Futagawa fault and Hinagu fault, respectively in the Beppu-Shimabara rift. Across the Futagawa fault the northern wall sank by one meter while the southern wall rose by 30 cm, and surface fractures and cracks along the fault zone are recognized.

After the quake, the field investigation of ground waters and hot springs around the faults have been carried out to detect a change in ground water by the earthquakes (e.g. Sato et al., 2017). They reported increased flow rate at several springs and newly occurred spring after the earthquakes, suggesting that the earthquake strongly affected the ground water system. Here we measured radon concentration in groundwater covering the sampling points of Sato et al. (2017).

Groundwater radon concentration changes have been reported as precursory indicators of earthquakes (e.g. Noguchi and Wakita, 1977; Kuo et al., 2006, 2011). Radium in rocks decays to produce radon and the radon is released from rock surface to pore. The rate of the radon release increase with the surface area, therefore the radon release can be indicative of the crustal deformation such as earthquake. Three significant radon anomalies relating to the 1978 Izu-Oshima-Kinkai earthquake (Wakita et al., 1980), the 1995 Kobe earthquake, (Igarashi et al., 1995) and the 2011 Tohoku earthquake (Tsunomori and Tanaka, 2014) have been reported in Japan. Tsunomori et al. (2017) also reported high groundwater radon concentration near active Tachikawa fault zone. These results imply that information of the underground deformation and structure can be acquired through radon in groundwater.

We report the results of groundwater radon concentration at 7, 11, 13 and 14 months after the 2016 Kumomato earthquake. In Kumamoto area, fortunately groundwater radon had been measured in 2009, seven years before the Kumamoto earthquake (Tokunaga, 2010). We then discuss the change of groundwater radon concentration in relation to the fault rupture by comparing our data to Tokunaga (2010), i.e. before and after the quake.

The results of our measurement show that the groundwater radon indicate high concentration in the step and jog region of Futagawa and Hinagu faults both before and after the earthquake. The concentration around newly recognized surface fracture is significantly high. Although there is a difficulty in comparing the radon data directly with those from the previous work gained by different measurement device, the radon concentration around southern-west of the faults drastically decreased. After the decrease, the concentration slightly increased, which may suggest a recovery of the concentration.

The change of groundwater radon concentration could be explained by the conservation equation for radon in a fracture system as (1) change in saturation ratio, or (2) change in specific surface area and/or porosity. The large decrease can’t be explained by change in saturation ratio, but accounted for change in porosity or specific surface area.

References

Sato et al., 2017, JpGU-AGU Joint meeting 2017.

Noguchi and Wakita, 1977, JGR 82, 1353-1357.

Kuo et al., 2006, Ground Water 44, 642-647.

Kuo et al., 2011, Nat. Haz. 59, 861-869.

Wakita et al., 1980, Science 207, 882-883.

Igarashi et al., 1995, Science 269, 60-61.

Tsunomori and Tanaka, 2014, Radiation Measurement 60, 35-41.

Tokunaga, 2010, Bachelor's degree thesis, Kumamoto University

NOTES

Pre-seismic anomalous observations before large earthquake in Taiwan: Insight from CWB geophysical data

Min-Chien Tsai[1*]

1. Seismological Center, Central Weather Bureau, Taiwan.
(minchyen@scman.cwb.gov.tw)

The Central Weather Bureau (CWB) build the Taiwan Geophysical Observation Network for monitoring the possible precursor signals. We analysis like groundwater data, earth tide, magnetic-filed data and the most famous is GNSS network. Wherein, we can use GNSS data to calculate the Total ionosphere total electron content (TEC), or using baseline variations of high-quality continuous GPS (cGPS) data. In this study, we characterize the possible pre-seismic precursor signal of two earthquakes in Taiwan. A significant decrease in extension rate was observed about 5 months before the M_L = 6.4 Rueisuei earthquake located near the Longitudinal fault of eastern Taiwan on 31 October 2013. A significant increase in soil-gas concentrations was also recorded 2 months before the Rueisuei earthquake. The pre-seismic baseline variation of cGPS was observed in 8 baselines near the epicenter of the M_w 6.4 Meinong earthquake located in the fold-and-thrust belt of SW Taiwan on 6 February 2016. In this case, we found clearly anomalous phenomenon in time series of 8 baseline length variations which the deformation rate was slowed down and decreased to near zero before Meinong earthquake. The duration of the anomalies are about 9 months to 2 year, depends on the location of baselines. Obviously, the duration time of anomalies is correlated to the distances of baseline location and epicenter. The dilatancy–diffusion model suggested that the pre-slip strain anomaly and could be observed on three major stages: elastic strain buildup (stage I), dilatancy dominant (stage II) and influx water dominant (stage III). Seismic slip may nucleate on fault patches due to the frictional drops with increasing slip or sliding speed, earthquake may occur on along-strike or downdip extension while aseismic deformation rates accelerate. However, according to dilatancy–diffusion model, the observed anomalies of baseline length rate variation seem to be "slow-down" and resulted from the closure of preexisting cracks before the nucleation of Meinong earthquake.

Keywords: GNSS, precursor, Central Weather Bureau.

NOTES

Agenda Sep. 6 (Wed)

TIME	PROGRAM		
08:00~09:00	Registration		
Session-5 *(host: Norio Matsumoto & Wen-Chi Lai)*			
TIME	**SPEAKER**	**TOPIC**	**PAGE**
9:00~9:20	Naoji Koizumi	Postseismic groundwater changes in and around the source region of the 2016 Kumamoto earthquake	59
09:20~9:40	Yasuhiro Asai	Step-like and exponential pore pressure/groundwater level changes associated with the 2016 Kumamoto Earthquake (Mj7.3) observed at Tono region, central Japan	63
9:40~10:00	Jyr-Ching Hu	Transient deformation induced by groundwater change in Taipei metropolitan area revealed by high resolution X-band SAR interferometry	65
10:00~10:20	Yasuyuki Kano	Groundwater anomalies recorded in historical documents	67
10:20~10:40	Wen-Chi Lai	The similarity of the coseismic groundwater level changes between 2016 Meinong Earthquake with 1999 ChiChi Earthquake	69

10:40~11:00	**BREAK & POSTER SESSION**

Agenda Sep. 6 (Wed)

TIME	PROGRAM		
Session-5 *(host: Jyr-Ching Hu & Yuzo Ishikawa)*			
TIME	**SPEAKER**	**TOPIC**	**PAGE**
11:00~11:20	Jing-Yi Lin	Application of Short Period Ocean Bottom Seismometer in Studying Marine Seismicity and Meteorological Environment	71
11:20~11:40	Pei-Yang Lin	Development and Application of Hybrid EEWS for schools and plants	75
11:40~12:00	Yi-Ying Wen	Aftershock evolution for the 2013 Ruisui and 2014 Fanglin earthquakes	77
12:00~12:20	Nai-Chi Hsiao	Current Status and Perspective for Felt Earthquake Information Reporting at CWB in Taiwan	79
12:20~12:30	**Closing Ceremony**		

Postseismic groundwater changes in and around the source region of the 2016 Kumamoto earthquake

Naoji Koizumi*[1], Tsutomu Sato[2], Hiroshi Takahashi[2], Norio Matsumoto[2],Kuniyo Kawabata[3], Takumi Ajiki*[1] and Azumi Mori*[1] ,

1. School of Environmental Science, the University of Shiga Prefecture
2.AIST, Geological Survey of Japan, Institute of Earthquake and Volcano Geology
3. Kagoshima University

The 2016 Kumamoto earthquake started with an M6.5 event (foreshock) on April 14. 28 hours after the foreshock, the main shock of M7.3 occurred on April 16. There were also many aftershocks. These earthquake series caused severe damage mainly in Kumamoto Prefecture in Japan. The foreshock and the main shock caused groundwater changes not only in the source region but also in the Shikoku, Kinki and Tokai regions, which are far from the source region(Koizumi et al.,2016). This time we will report the postseismic groundwater changes in Kumamoto Prefecture.

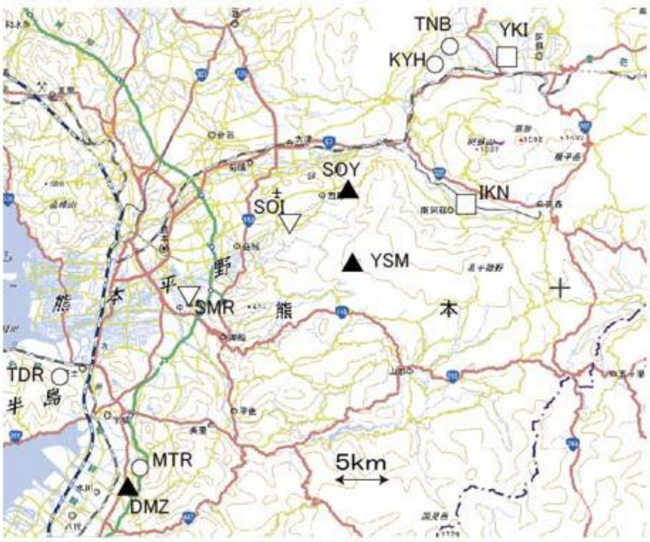

Fig.1 Sampling sites of the spring waters.
○:No flow rate data before the 2016 Kumamoto earthquake. □:No flow rate change before and after the main shock, ▽: Flow rate drop just after the main shock, ▲:Flow rate rise just after the main shock. The background map was obtained from the web page of Geospatial Information Authority of Japan (2017).

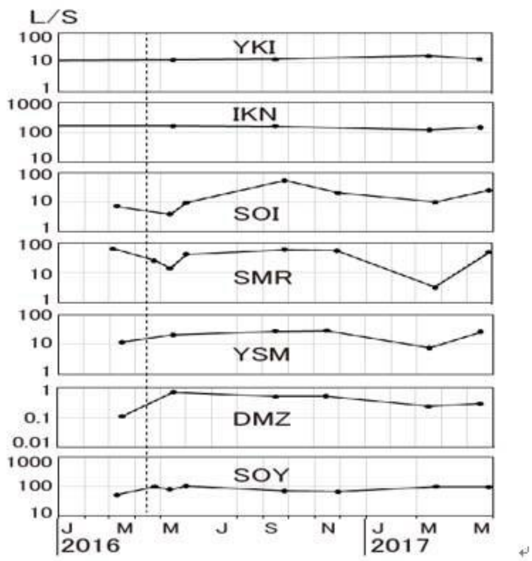

Fig.2 Temporal flow rate change in the seven spring waters (Fig.1) where there were the flow rate data before the 2016 Kumamoto earthquake. The dotted line shows the occurrence of the foreshock and the main shock.

We surveyed 11 spring waters shown in Fig.1 four to seven times after the main shock. We generally measured flow rate, temperature and chemistry of those spring waters. We also surveyed eight of the eleven spring waters before the 2016 Kumamoto earthquake although we did not measure the flow rate of one of the eight springs before the 2016 Kumamoto earthquake. Therefore we can evaluate the postseismic hydrological and chemical changes at the eight spring waters (Sato et al.,2017).

Fig.2 shows the temporal flow rate change in the seven spring waters during the period from January 2016 to May 2017. Just after the main shock, the flow rate was increased at the three spring (YSM, DMZ, SOY), decreased at the two spring (SOI, SMR) and not changed in the two spring (YKI,IKN) (Figs.1 and 2). At YKI and IKN the flow rate has also been stable since the main shock. At SOI and SMR the flow rate has been changed largely since the main shock. Therefore we cannot judge whether the drop of the flow rate just after the main shock was caused by the earthquake or not. At YSM, DMZ and SOY, the flow rate seemed to return to the value which was measured before the 2016 Kumamoto earthquake. However recently the flow rate tends to be increased at YSM, DMZ and SOY. In the presentation, we will report the postseismic hydrological changes in detail and discuss factors for the different patterns of them.

References

Geospatial Information Authority of Japan, 2017, Maps of Geospatial Information Authority of Japan, http://maps.gsi.go.jp/.

Koizumi,N., T. Sato, H. A. Takahashi and N. Matsumoto, 2016, Groundwater changes related to the 2016 Kumamoto earthquakes, 15th Japan-Taiwan International Workshop on Hydrological and Geochemical Research for Earthquake Prediction, Tsukuba, Japan, September 2016.

Sato, T, H. A. Takahashi, K. Kawabata, M.Takahashi1, Y. Tosaki, A. Miyakoshi, A. Inamura, H. Handa, N. Matsumoto, K. Kazahaya, 2017, Anomalous changes in groundwater and hot spring water after the 2016 Kumamoto earthquake, JPGU-AGU Joint meeting 2017, Chiba, Japan, May 2017.

Step-like and exponential pore pressure/groundwater level changes associated with the 2016 Kumamoto Earthquake (Mj7.3) observed at Tono region, central Japan

Yasuhiro Asai[1*], Hiroshi Ishii[1] and Osamu Murakami[1]

1. Tono Research Institute of Earthquake Science, Association for the Development of Earthquake Prediction

The 2016 Kumamoto Earthquake (Mj7.3) occurred at the Kyushu, southwest Japan at 01:25 (JST), 16 April 2016. Clear exponential pore pressure/groundwater level changes associated with this earthquake were observed at STG200 and STG200N borehole observation sites in Mizunami Underground Research Laboratory (MIU), and TGR350 borehole observation site located approximately 500m south of MIU, in the Tono region, central Japan (Hypocentral distances are approximately 665km). Pore pressure increases in STG200 and STG200N and groundwater level rise in TGR350 reached a peak at 5 June, 2016, respectively, after that, these changes became a downward trend. The peak amplitude of pore pressure changes in STG200N and STG200 are 30 and 28 kPa, respectively and groundwater level in TGR350 is 2.3m. Although those are different features, co-seismic pore pressure /groundwater level changes were also observed at STG300 site in MIU and SBS105 site located approximately 1km north-west of MIU. In addition, Pore pressure increases and groundwater level rise were observed at 1 April 2016 (Mj6.5, Southeast off Mie Prefecture Earthquake) and 21 October, 2016, but no groundwater level change was observed at SBS105 (Mj6.6, Central Tottori Prefecture Earthquake).

At the STG200N site, continuous in-situ stress recorded by the borehole stress meter (Ishii and Asai, 2015; EPS). In order to recognize the relationship between the co-seismic pore pressure changes and the seismic waves, we compared the 20 Hz sampling pore pressure and stress records before and after the occurrence of 2016 Kumamoto Earthquake (Mj7.3). Dynamic stress and pore pressure variations were observed at approximately 01:29 (JST), 16 April 2016. The maximum peak-to-peak amplitude of dynamic stress variations were 20.2 kPa (N324E) to 59.1 kPa (N54E), and those of pore pressure variations were 92.4 kPa in STG200N and 55.5 kPa in STG200. As the result, pore pressures begin to increase just after the maximum amplitude of seismic waves (dynamic stress variations) passed through our site.

It is interesting that co-seismic pore pressure steps were observed at STG200N and STG200, but no groundwater level step was observed at TGR350. The amplitude of steps are +6.3 kPa and +4.3 kPa at STG200N and STG200, respectively. In other words, steps of STG200N is 1.5 times larger than STG200. In order to recognize whether differences are exists for STG200N, STG200 and TGR350 during non-earthquake conditions, we compared the tidal parameters on pore pressure and groundwater level records. The results for the main tidal waves show tidal responses of these observation sites are coincide with each other, in other words, the difference in response during non-earthquake conditions does not exists.

We will present the details of these pore pressure/groundwater level changes, and attempt to clarify the qualitative/quantitative model for the co-seismic pore pressure/groundwater level changes.

Transient deformation induced by groundwater change in Taipei metropolitan area revealed by X-band SAR interferometry

Jyr-Ching Hu[1*], Hsin Tung[1], Pei-Juin Wu[1], Horng-Yue Chen[2]

1. Department of Geosciences, National Taiwan University.
2. Institute of Earth Sciences, Academia Sinica
(jchu@ntu.edu.tw)

We present precise deformation velocity maps for the two years period from September 2011 to July 2013 of the northern Taiwan area, Taipei, by using persistent scatterer interferometry (PSI) technique for processing 18 high resolution X-band synthetic aperture radar (SAR) images archived from COSMO-SkyMed (CSK) constellation. According to the result, the highest subsidence rates are found in Luzou and Wuku area in which the rate is about 15 mm/yr and 10 mm/yr respectively in the whole dataset. However, dramatic change from serve subsidence to uplift in surface deformation was revealed in the Taipei Basin in two different time spans: 2011/09–2012/09 and 2012/09–2013/07. This result shows good agreement with robust continuous GPS measurement and precise leveling survey data across the central Taipei Basin. Moreover, it also represents high correlation with groundwater table. This high correlation indicated that one meter groundwater level change could induce about 8 and 16 mm surface deformation change in Luzou and Wuku area respectively, which is about eight times faster the long-term tectonic deformation rate in this area. Thus, to access the activity of the Shanchiao Fault, it is important to discriminate tectonic movement from anthropogenic or seasonal effect in Taipei Basin to better understand the geohazards and mitigation in the Taipei metropolitan area.

Keywords: InSAR, land subsidence, GPS, leveling.

Groundwater Anomalies Recorded in Historical Documents

Yasuyuki Kano[1*]

[1] Disaster Prevention Research Institute, Kyoto University, Japan

Groundwater anomalies associated with large earthquakes are frequently recorded in historical documents. It seems that people kept recording the status of groundwater such as amount and quality because of the importance of ground water as water resource. The records are appeared in diaries, letters, essays and so on. Most of the articles reported on anomalies occurred in groundwater wells and hot springs. Those articles, in general, seems to have been honesty record what occurred before and after the earthquake. However, we also need to carefully examine the records if there were confusions or miswriting and if there is exaggerated expressions.

Wakita (1978) made a list of the articles that records of groundwater anomalies before and after the earthquakes appeared on from historical documents in Japan. The list was made basically from *Dai-Nihon Jishin Shiryo* (Collection of Historical Documents on Earthquakes in Great Japan) (Tayama, 1904a,b) and *Zotei Dai-Nihon Jishin Shiryo* (Collection of Historical Documents on Earthquakes in Great Japan, Enlarged and Revised Edition) (Musha, 1941, 1943a,b). From 1979 the effort to collect historical earthquake documents started, which leads to publication of *Shinshu Nihon Jishin Shiryo* (Historical Documents on Earthquakes in Japan, New Collection) (Earthquake Research Institute of the University of Tokyo, 1981-1994).

In *Shinshu Nihon Jishin Shiryo*, huge numbers of historical earthquake documents are collected. The documents include the articles that record the groundwater anomaly associated with earthquakes. In this report, a new list of groundwater anomalies recorded in historical documents are presented. Some of the listed groundwater anomalies are analyzed or interpreted applying modern understandings of earthquake hydrology. Groundwater anomalies can be generally explained by static strain steps or dynamic strain oscillations i.e. seismic waves.

Articles on groundwater anomalies are newly identified in historical documents owned by National Taiwan University. The documents are written at Wakayama, Japan, in 1850s and records what occurred at the times of 1830 Kyoto earthquake ans 1854 Ansei Nankai earthquake and tsunami in around Wakayama. The articles are also included in the discussion.

The similarity of the coseismic groundwater level changes between 2016 Meinong Earthquake with 1999 ChiChi Earthquake

Wen-Chi LAI[#+], Shih-Jung WANG, Kuo-Chin HSU, Chjeng-Lun SHIEH

National Cheng Kung University, Taiwan
[#]*Corresponding author: laiwenji@dprc.ncku.edu.tw* [+]*Presenter*

The different response by various natural stimuli and processes (tidal force, barometric loading, ground shaking and crustal strain) were used as the elements of the hydraulic information in the earthquake induced groundwater level changes. Using the natural force to act as naturally recurring stimuli to provide a sufficiently varied distribution of excitations in time and space, and represented the hydro-geological changes responses to the earthquake processes. The purposes of this study are to analyze the recently observation results of the earthquake induced pre-seismic / co-seismic variation of groundwater level ML 6.4 Tainan earthquake, Feb. 6th 2016. The analysis of the high-sampling water level responses be used to estimate the mechanical properties of the aquifer. Comparison the observation high-sampling water level changes in the each event, offers the opportunity to discussion the possible mechanism of the hydrologic response to earthquake. Some of the coseismic groundwater level changes can be explained as the poroelastic responses to the earthquake-induced volumetric strain changes inferred from the fault dislocation models. But the other changes can not be explained by the volumetric strain changes either qualitatively or quantitatively. We regarded the coseismic static volumetric strain change and the ground acceleration as the main factors to cause the coseismic groundwater level changes. The study provides some information for the pre-seismic / co-seismic mechanism but more investigations are required.

Application of Short Period Ocean Bottom Seismometer in Studying Marine Seismicity and Meteorological Environment

Jing-Yi Lin[1*], Yen-Fu Chen[1], Shao-Jin Chin[1], Yi-Chin Lin[1] and Chin-Wei Liang[1]

1. Department of Earth Sciences, National Central University, Taiwan.
(jylin.gep@gmail.com)

Ocean-bottom seismometers (OBSs) have been widely used over the past decades to collect seismic data for seismic monitoring of the ocean floor, exploitation of oil and gas hydrates, and detection of tsunamis. However, OBSs detect more than just earthquakes and active seismic sources. Many other events, such as meteorite impacts and nuclear explosions, can produce distinctive vibrations in the Earth's crust that appear in seismic records. In addition, OBSs are now widely used to observe myriad low-frequency submarine events, such as submarine volcano activity and seafloor monitoring. Various types of OBS have been deployed in the waters around Taiwan with different scientific goals since 1991. Nowadays, Taiwan has its own self-designed OBS and several OBS pools are ready for use. Among them, the short period type OBS possessing small size, light weight, is suitable for the deployment for small vessels. Here we introduce several examples for the application of short period OBS in Taiwan and some of them are unconventional.

(1) Studies in tectonic problems: located at the arc-continental collision region between the Eurasian (EP) and Philippine Sea Plates (PSP), Taiwan is usually considered to have a complex tectonic environment, particularly along the eastern coast of the island. To gain a better understanding of the geological evolution of the east Taiwan area, the data from 8 OBSs acquired during the Across Taiwan Strait Explosion Experiment in 2012 and 14 inland seismic stations were used to determine a more detailed and accurate distribution of marine earthquakes. Based on the 333 relocated earthquakes and available geophysical data, we suggest two main tectonic boundaries for eastern Taiwan (Fig. 1). South of 23.25°N, the homogeneous distribution of earthquakes in the crustal portion for both the inland and offshore areas suggests an ongoing collisional process. North of this location, between approximately 23.25°N and 23.8°N, the abrupt increasing of seismicity depth infers that the underthrusted arc/fore-arc material is deforming due to the collisional compression at depth. In this segment, the subsidence of the arc/fore-arc area determines the transition from collision to subduction. North of 23.8N, the northwestern dipping PSP is well illustrated by the seismicity both onshore and offshore, indicating a dominant subduction process.

(2) Studies in meteorological condition: From the end of August to early September 2011, 15 OBSs were deployed offshore northeastern Taiwan for approximately 20 days. During this period, the typhoon Nanmadol formed in the western Pacific, moved northwestward from the East Philippines, and made landfall on the island of Taiwan. In this study, we analyzed the seismic signals from the OBSs and the marine metrological data to investigate the influence of the typhoon on submarine

seismic records. Our results show that the signals induced by the typhoon occurred mainly at approximately 0.15–0.5 Hz frequency (Fig. 2). The magnitude of these signals depends substantially on water depth. Also, a positive correlation exists between the signals energy and the local wave height, which suggests that the microseisms were affected by the pressure changes produced by the local wave activity as the typhoon passed over the stations. However, when an OBS was outside the typhoon periphery, any wave energy variations could only be caused by the elastic wave formed around the typhoon area, the energy of which is transmitted through the ocean bottom to the stations. Thus, no local waves were excited by the strong winds, and only a relatively small amount of energy was recorded.

(3) Short duration events (SDEs): SDEs signal has characteristics that are very different from those produced by tectonic earthquakes, e.g.: durations < 1 s, frequencies between 10 and 30 Hz, and one single-wave trains, with no identified P- nor S-wave arrivals. SDEs are commonly found and could be due to gas expulsions from the seafloor and biological activity. To discriminate between the 2 hypotheses, seismic recordings combined with video surveillance have been made. In May 2016, two OBS (4.5 Hz) were deployed offshore Molene Island, Brittany within the field of view of the EMSO-Molene underwater observatory, at a water depth of 12 m (Klingelhoefer et al., AGU abstract, 2016). The camera images and the recordings reveal the presence of crabs, octopus and several species of fish, which show relatively complex waveform signature. However, by performing the cross-correlation work for the seismograms obtained form an OBS network around the MV1 area, located SW offshore Taiwan, the similarity of the waveform size and appearance indicates that the degassing effect thought the same conduit could be the origin of these SDEs (Fig. 3). This result could be helpful for the quantification of the shallow-ocean methane of carbon-dioxide leakage to the atmosphere.

Keywords: Ocean Bottom Seismometer, wave height, typhoon, microseisms, short duration events, gas expulsion

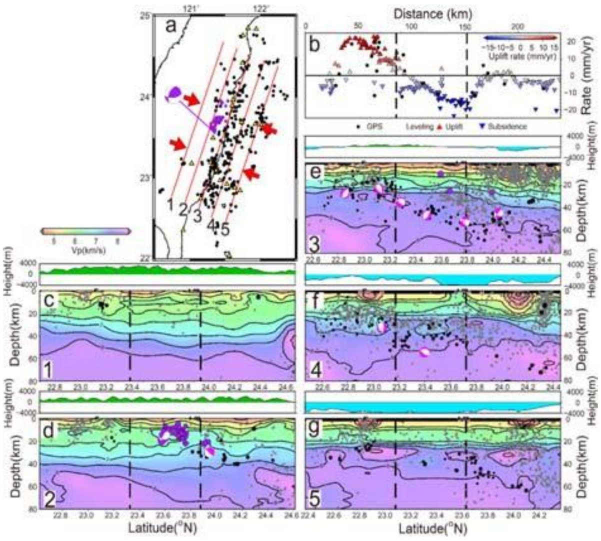

Figure 1. The relocated earthquake distribution along the five NE-SW cross-sections located from the inland to offshore area. (a) Profile locations (red lines) and the relocated earthquakes (black dots) in plan view. (b) Leveling and continuous GPS data extracted from Ching et al. (2011). The uplift and subsidence rate calculated from the leveling experiment are shown by triangles with red and blue colors, respectively. Black dots show the vertical velocity estimated from GPS data. (c)–(g) Are the seismic tomographic results and the relocated earthquakes along the five profiles 1–5 in (a). Gray dots show the earthquakes from the reviewed ISC catalog. Black dash lines indicate two tectonic boundaries. Black triangles denote the OBS positions. Purple dots and focal mechanism represent the Ruisui sequence. The pink focal mechanisms are obtained from our study.

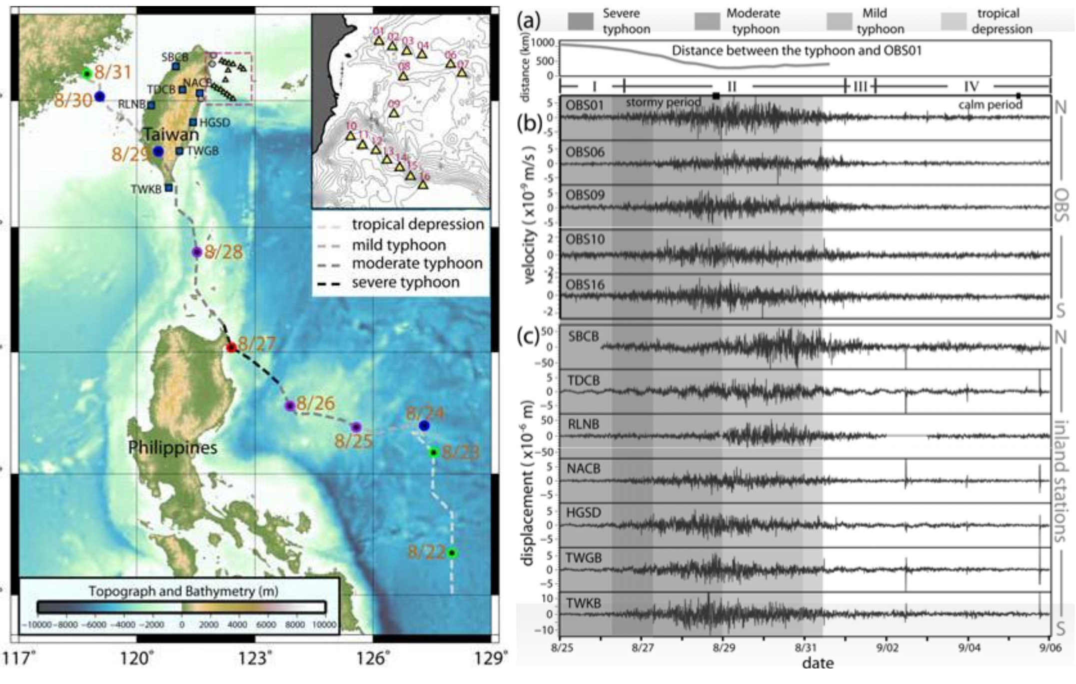

Figure 2. (Left) Regional bathymetry with the center track of the typhoon Nanmadol. Triangles show the positions of ocean-bottom seismometers (OBSs), and squares show the positions of the inland broadband stations selected from the Broadband Array in Taiwan for Seismology (BATS) network. The wave buoys are, from north to south,

Londong, Kueishantao, and Hualien, and are indicated by dots. Typhoon intensity is marked by the shading of the dashed lines. The inset shows the configuration of the array of 15 fourcomponent, short-period OBSs. (Right) Seismograms recorded at different stations. (a) The distance between OBS01 and the center of the typhoon Nanmadol. Waveform data from the vertical component of the OBSs and some selected inland BATS stations with a 1 Hz low-pass filter applied are shown in (b) and (c). Different typhoon intensities are represented by zones of different shading. The symbols I, II, III, and IV indicate the time windows that we used for the analyses in Figure 7. The two black bars on the top of (b) show the two times that we used to define the stormy period and the calm period.

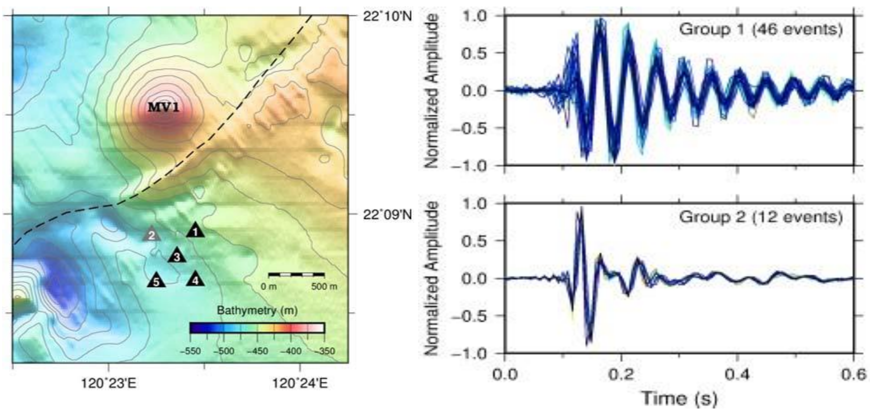

Figure 3. (Left) OBSs location. MV1 is a submarine volcano. (Right) Examples of SDE waveforms between two different groups, The waveform of the same group show very good consistency.

Development and Application of Hybrid EEWS for schools and plants

Pei-Yang Lin1[1*]

1. National Center for Research on Earthquake Engineering
200, Sec. 3, Xinhai rd., Taipei, Taiwan, R.O.C.
(pylin@narlabs.org.tw)

National Center for Research on Earthquake Engineering (NCREE) started to develop the Earthquake Early Warning System (EEWS) from 2009. In the past years, several earthquake early warning algorithms had been developed, the integrated on-site EEWS had been validated through the shaking table tests and long-term in-field tests. There were more than 30 on-site EEWS demonstration sites had been established for the past six years. Through hundreds of the earthquakes in these years, the proposed on-site EEWS had been refined and validated to be effective to provide tens of seconds of warning time before the main shaking. From 2013, NCREE combined the regional EEW from CWB and the proposed on-site EEW to develop the hybrid EEWS for schools and plants. The hybrid EEWS can provide longer warning time for both far-field and near-field earthquake. The EEW alarm was also connected to the broadcast system in schools, and been tested in the seismic disaster prevention drill to help people to known how to use it. In the same time, NCREE also presented the customized EEW for plant, which can provide several predicted PGA levels o help the plant to setup several disaster prevention control scenarios, to dramatically reduced the economic loss due to earthquake.

TE

Aftershock evolution for the 2013 Ruisui and 2014 Fanglin earthquakes

Yi-Ying Wen[1*]

1. Department of Earth and Environmental Sciences, National Chung Cheng University, Taiwan
(yiyingwen@ccu.edu.tw)

The NNE-trending 150-km-long Longitudinal Valley fault (LVF), which overlies the suture zone between the Philippine Sea plate and the Eurasian plate, is an active thrust fault. In the past, the Longitudinal Valley has been struck by several large events, e.g., the 1951 Longitudinal Valley earthquake sequence and the 2003 Cheng Kung earthquake. On October 31, 2013, the ML 6.4 Ruisui earthquake struck the northern segment of the LVF. Based on the background seismicity from the past two decades, it is noted that the epicenter of the 2013 Ruisui event is located in a seismic gap, where there is an unclear segment between the locked zone in the north and the creeping fault in the south. Seven months later the May 21, 2014 Mw 5.6 Fanglin earthquake occurred at the northern end of the 2013 Ruisui event aftershock distribution. Considering the limitation of seismic station coverage, we apply matched filter technique to detect the ignored microearthquake of the aftershock sequence for the 2013 Ruisui and 2014 Fanglin events and obtain the complete seismic catalog, which could help to investigate the spatial and temporal variation of seismicity, the mechanisms of seismic activity and seismogenic structures and providing useful information on seismic hazard assessment in the future.

Keywords: 2013 Ruisui earthquake, 2014 Fanglin earthquake, aftershock sequence

TE

The International Workshop of Technology of Earthquake Monitoring and Geophysical data Analysis Application & The 16th Japan-Taiwan International Workshop on Hydrological and Geochemical Research for Earthquake Prediction - *oral*
Sep. 5-6, 2017

Current Status and Perspective for Felt Earthquake Information Reporting at CWB in Taiwan

Nai-Chi Hsiao[1*], Wen-Chi Hsiao[1], Da-Yi Chen[1], and Chiao-Ying Lee[1]

1. Seismological Center, Central Weather Bureau, Taiwan.
(naigi@scman.cwb.gov.tw)

Taiwan is located on the border of the Eurasian Plate and the Philippine Sea Plate, part of the Circum-Pacific seismic belt. Earthquake is one of the most threatening natural disasters in Taiwan. Averagely 40,000 seismic events detected every year, and nearly 500 earthquakes are felt ones among them. Therefore, the tight earthquake monitoring and valuable information reporting for seismic hazard mitigation and related research offer is very important and necessary. Over the past decade, the Central Weather Bureau (CWB) of Taiwan has upgraded the seismic network CWBSN (Central Weather Bureau Seismographic Network). The recording capability of instruments and site condition of stations are both improved. Based on the CWBSN, kinds of felt earthquake information are reporting. Currently, while a potentially felt earthquake is occurring around Taiwan area, an automatic report include earthquake location and magnitude can be obtained in about one minute. Then, a brief shake map with areas greater than Taiwan Seismic Intensity 4 (PGA>25 gal) can be provided to the emergency management agency in about 2 minutes. Within 3 to 5 minutes later, an official earthquake report is disseminated to various organizations and individuals. In order to provide an early warning of seconds to tens before the strong shaking arrival, the reporting for earthquake early warning was developed and operated. Currently, for earthquakes occurring in or very near Taiwan, information can be automatically reported in about 15 seconds averagely. Hence, it can offer early warnings before the S-wave arrival for the metropolitan areas located at 50 km away from epicenter. Recently, the earthquake early warning has started to disseminate for the public through the Internet, Cell Broadcast (CB) on mobile device, and TV. Furtherly strengthen the effectiveness of earthquake information after the felt earthquake occurrence in Taiwan.

Keywords: felt earthquake, earthquake rapid reporting, earthquake early warning.

The Posters

CGS: Central Geological Survey, MOEA, Taiwan.

NTU: National Taiwan University, Department of Geosciences, Taipei, Taiwan.

SCCWB: Seismological Center, Central Weather Bureau, Taipei, Taiwan.

SPU: School of Civil Engineering and Architecture, Southwest Petroleum University, Chengdu, China.

No.	PRESENTER	TOPIC	PAGE
P08	Hsin-Chieh Pu (SCCWB)	Spatial and temporal characteristics of the microseismicity preceding the 2016 M_L 6.6 Meinong earthquake in southern Taiwan	99
P09	Ying-Hui Yang (SPU)	Shallow fault rupture triggered by main shock of the 2016 Meinong earthquake inferred by Multi-sight InSAR and GPS data	101
P10	Pei-Chin Wu (NTU)	Characterizing the deformation pattern of Mass Rapid Transportation in Taipei basin by SAR interferometry	103
P11	Da-Yi Chen (SCCWB)	Citizen Seismology for Earthquake Early Warning System	105
P12	Tz-Shin Lai (SCCWB) (NTU)	A Study of Site Effect on Station Corrections of Magnitude and Measurement of the Spectral Decay Parameter Kappa Using Borehole Seismic Array Data	107
P13	Yi-Ching Lo (NTU)	Developing a Near Real-time Automatic System for Rupture Inversions of Moderate and Large Earthquakes	109

CGS: Central Geological Survey, MOEA, Taiwan.

NTU: National Taiwan University, Department of Geosciences, Taipei, Taiwan.

SCCWB: Seismological Center, Central Weather Bureau, Taipei, Taiwan.

SPU: School of Civil Engineering and Architecture, Southwest Petroleum University, Chengdu, China.

Estimation of barometric pressure response in borehole strainmeter with typhoon events in Taiwan

Chun-Ying Chiu[1], Jyr-Ching Hu[1*], and Chi-Ching Liu[2]

1. National Taiwan University, Department of Geosciences, Taipei, Taiwan
2. Institute of Earth Sciences, Academia Sinica, Taipei, Taiwan
(jchu@ntu.edu.tw)

Taiwan is located in an active collisional boundary of Philippine Sea plate and Eurasian plate in a convergence rate of _82 mm/yr, which results in high frequent seismicity and destructive big earthquakes. In order to monitor the strain change from pre-slip events, 13 Gladwin Tensor Strainmeters (GTSM) were installed in a depth of _200 m in western Foothills of Taiwan since 2003. The previous studies demonstrated that the broad environmental signs of barometry, rainfall, tide and groundwater should be calibrated to detect the tectonic signal. The previous study from borehole strainmeter of PBO in western US suggested that the strainmeter gauge time series were divided into records of approximately 60 days, overlapping when possible by 30 days. In order to determine the barometric pressure response of each gauge, the gauge outputs and atmospheric pressure data were band-pass-filtered to exclude frequencies outside the 4–6 day band. The results showed that sixty day records had a good correlation between the atmospheric pressure and the strainmeter gauge time series. Due to the climatic characteristics of annual rainfall could reach to 2500 mm in Taiwan, the long duration of gauge time series will be distributed by rainfall signal. Thus we suggest to divide the gauge time series records of approximately 30 days, overlapping when possible by 5 days. A good correlation of between the atmospheric pressure and the strainmeter gauge time series were identified by using a band-pass-filtered to exclude frequencies outside the 3–7 day band. In addition, we can use the linear regression from gauge time series and barometric drop due to the before the typhoon events with no interference of rainfall events. The average atmospheric pressure response coefficients of the strainmeters are about -0.14_-0.38 _strain/KPa.

Keywords: borehole strainmeter, barometric pressure response

NOTES

Using Independent Components Analysis to diminish the response of groundwater in borehole strainmeter

Chih-Yen Chen[1,2*], Jyr-Ching Hu[2]

[1] Central Geological Survey, MOEA, Taiwan, ROC
[2] Dept. Geosciences., National Taiwan University, Taiwan, ROC
(zychen@moeacgs.gov.tw)

With designed feature, borehole strainmeter can not only record minor signals of tectonic movements, but also broad environmental signs such as barometry, rainfall and groundwater. Among these external factor, groundwater will influence the observation of borehole strainmeter mostly. According essential observation, groundwater will cause much bigger response than the target strain change - tectonic strain. We sited transducers to record pore pressure of groundwater in the rock formation. Then compare strain result to obtain the relationship of both. But there still exist some problems that have to be solved. First, due to instrument limitation, we couldn't set the pore-pressure transducer in the same aquifer as strainmeter did. In this case, the result will be expected can't represent the pore pressure exactly. Furthermore, problem of electricity and connectivity in station will cause the record lack and lost. Therefore, it's necessary to find out a better and more stable method to diminish the groundwater response of strainmeter data. Strain transducer with different orientation can observe the groundwater response in different scale. If we can extract out groundwater signal from each independent strain transducer and estimate its original source. That will significantly rise signal strength and lower noise level. Such case is some kind of blind-signal-separation, BSS problem. The procedure of blind-signal-separation extract or rebuild signal that can't be observed directly in many mixed sources and Independent Component Analysis, ICA is one method adopted broadly. ICA is an analysis to find out parts which have statistics independence and non-Gaussian factor in complex signals. We use FastICA developed by Hyvärinen (1999) to figure out the groundwater response strain in original strain data, and try to diminish it to rise the signal strength. We preceded strain data previously, then using ICA to separate data into serval independent components. Among them, we found one is highly correlated to groundwater result. It has not only good correlation in long-term trend, but also in short-term fluctuations. It can effectively minimize the groundwater response strain and highlight small signal of tectonic activities in borehole strainmeter data.

Keywords: borehole strainmeter, strain data analysis, independent component analysis, ICA, environmental response strain

NOTES

The application of present-day continuous GNSS network of the Central Weather Bureau

Yu-Ting Huang[1*], Bo-Kuan Li[1], Min-Chien Tsai[1], Yu-Hsiang Wang[1]

1. Seismological Center, Central Weather Bureau, Taiwan.
(r00241306@scman.cwb.gov.tw)

The Central Weather Bureau (CWB) began to set up a permanent Global Positioning System (GPS) continuous observation stations from 1994. After the Chi-Chi earthquake in 1999, the CWB found the importance of crustal deformation monitoring but the lack of continuous GPS (cGPS) stations in Central Taiwan Area. Therefore, the CWB participated in the interdepartmental integration plan "Earthquake and Active Fault Research" of Ministry of Science and Technology, and expand continuous GPS observation network year by year. The instruments were updated to Trimble NetR9 and began to receive the data of GLONSS, Galileo, and other satellite system after 2012. The cGPS observation network was upgraded to Global Navigation Satellite System (GNSS) to improve the precision of the measurement results. At the end of 2016, there were 160 continuous GNSS (cGNSS) observation stations (Figure 1) had been in operation.

All the cGNSS observation data are real-time received by ADSL and 3.5G communication, and also backup automatically. We use the “Translation, Editing, and Quality Check” (TEQC) software which is developed by UNAVCO to do data quality control by the figures of the site sky-plot and Quality Control Time Series. In terms of processing software, there are two sets of GNSS data solving systems in CWB. One is GAMIT/GLOBK which is developed by the Massachusetts Institute of Technology (MIT) and the University of California, San Diego, the Scripps Institute for Oceanography (Scripps Institute of oceanography, SIO). The other one is “GPS Inferred Positioning System / Orbit Analysis and Simulation Software” (GIPSY/OASIS), developed by Jet Propulsion Laboratory (JPL) of National Aeronautics and Space Administration (NASA). The GAMIT/GLOBK software solved data by the network adjustment technology of the relative positioning. The double difference method are used in elimination or reduce the satellite and receiver clock error, track error, troposphere, ionosphere and other systematic errors in GAMIT/GLOBK software. The GIPSY/OASIS software are different form GAMIT/GLOBK, the data is solved by Precise Point Positioning (PPP) technology. Two sets of software in the function of calculation and the results of the advantages and disadvantages are different. The preliminary results show the results of two software have the similar trend. There will be more results of discussion and compression in further study.

According to the elastic rebound theory (Reid, 1910), the earthquakes are caused by the rapid release of energy after the crust is squeezed producing energy accumulation due to the plate effect, therefore, the correlation between the crustal deformation and the earthquakes is important. We have abundant seismic data and geophysical data for this study in CWB. Hence, we attempts to compare the time series, velocity variation, and coseismic displacement of GAMIT/GLOBK and GIPSY/OASIS software. Exploring the possible causes of the differences and trying to correct the parameters to make sure the correctness of the results. Furthermore, the results in this study could help us understand more about the relationship between crustal and seismicity in Taiwan, finding out the possible anomalies before earthquake and serving as the basis for future seismic potential assessment.

Keywords: GNSS, continuous GNSS stations, GNSS data process

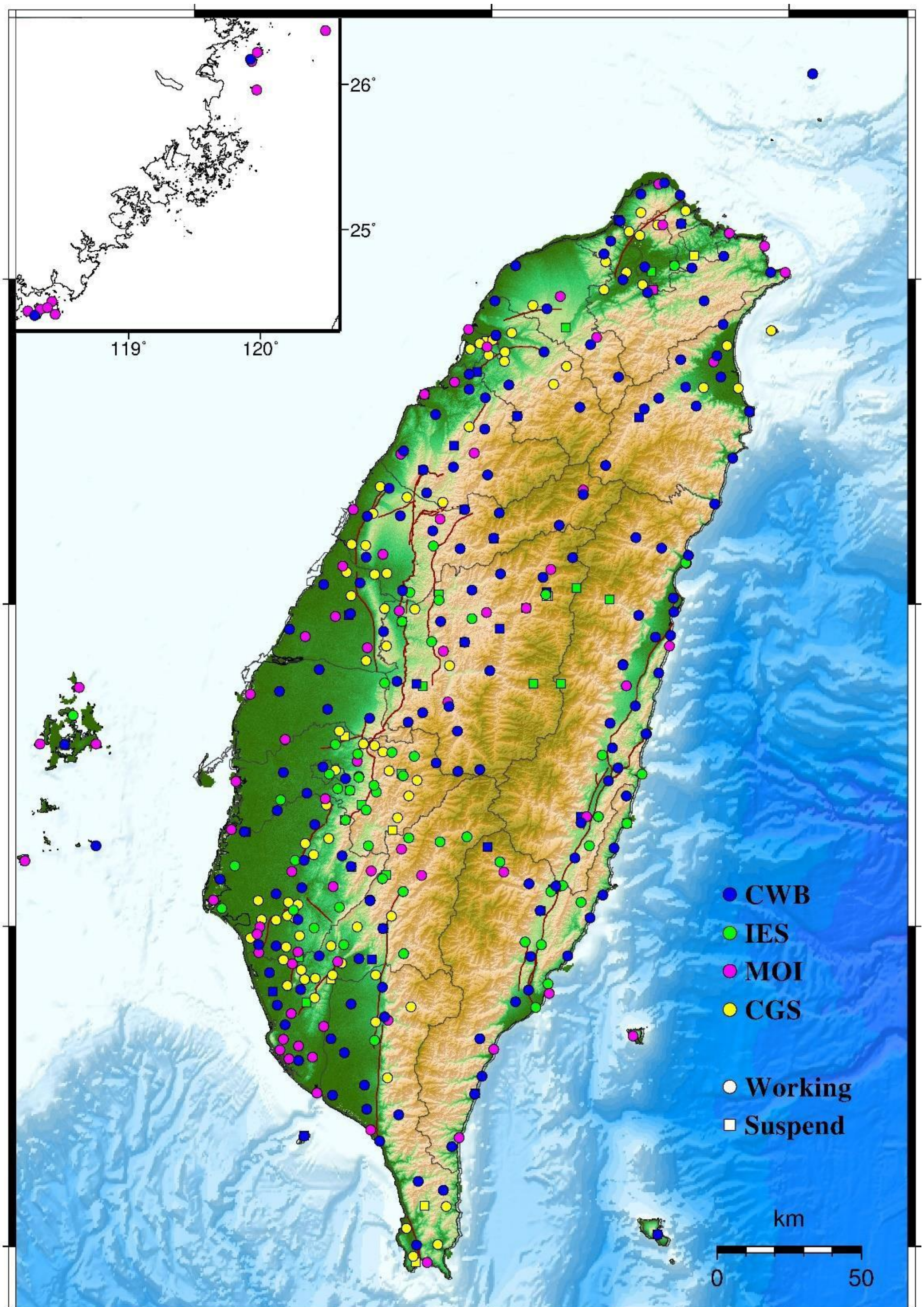
26°
25°
119°
120°
25°
24°
23°
22°
120°
121°
122°
CWB
IES
MOI
CGS
Working
Suspend
km
0
50

Fig. 1

NOTES

Development of GNSS Real-Time Streams Observation Network in Central Weather Bureau

Yu-Hsiang Wang[1*]

1. Seismological Center, Central Weather Bureau, Taiwan.
(b6100111524@hotmail.com)

Since 1994, the Central Weather Bureau (CWB) has started to set up permanent Global Positioning System (GPS) observation stations all around Taiwan. After the 921 Chi-Chi Earthquake in 1999, seismic disaster and surface deformation were becoming more important topics in Taiwan's earth science researches. Until 2016, the CWB had set up more than 150 GPS stations, which formed an observation network. In recent five years, the new generation of Trimble NetR9 could support multi Global Navigation Satellite System (GNSS) and improve data quality by which old instruments were replaced. With a stable data transmission on the ADSL (Asymmetric Digital Subscriber Line) internet, Trimble NetR9 could also transmit real-time GNSS data streams through the NTRIP (Networked Transport of RTCM via Internet Protocol) transport protocol. For these reasons, there were 100 ideal GNSS stations which would be integrated into the latest GNSS real-time streams observation network by BKG's software. The BKG Professional NtripCaster is the software which manage those real-time streams as an administrator developed by Bundesamt für Kartographie und Geodäsie (BKG), GNSS Data Center (GDC). Another software, BKG Ntrip Client (BNC), support to retrieve those real-time streams available through the NtripCaster, and carry out real-time Precise Point Positioning (PPP) to determine the positions of GNSS stations. In this study, we design an applicable process of real-time GNSS data streams, including standard operating procedures of GNSS stations increment, GNSS stations division, and streaming user permission management. On the other hand, the BNC settings have been going through a series of tests, such as solution analysis, quality analysis, real timing analysis, and stability analysis. In the future, the GNSS real-time data stream observing system will be brought into our geophysical observation work in CWB. Moreover, we will also plan related strategy of data disclosure in order to proactively cooperate with academia.

Keywords: GNSS, BKG Professional NtripCaster, BKG Ntrip Client, Real-time PPP, GNSS real-time data streams.

NOTES

The GPS data process and applications by GIPSY in Central Weather Bureau

Bo-Kuan Li[1*], Yu-Ting Huang[1], Min-Chien Tsai[1]

1. Seismological Center, Central Weather Bureau, Taiwan.
(jabberwock@scman.cwb.gov.tw)

The GNSS-Inferred Positioning System and Orbit Analysis Simulation Software (GIPSY/OASIS) is developed by the Jet Propulsion Laboratory (JPL) in The National Aeronautics and Space Administration (NASA) and processing GPS data by Precise Point Positioning (PPP) technique. The unique PPP technique can save GPS data processing time, in average, it only takes 24 hours to finish estimation the final daily solution for more than 400 continuous GPS (cGPS) stations. The efficient operation of GIPSY/OASIS is very useful when disaster earthquake happen. Therefore, the Central Weather Bureau (CWB) starts to apply GIPSY/OASIS software for cGPS data process.

The basic idea to obtain the high precision daily solution is setting the boundary constraint to avoid the outliers. The boundary constraint is the sigma value should be less than 1 cm form the result summary file named “Postfit.sum”. The summary file contacts the sigma errors, number of sampling points and outliers of ionosphere-free carrier phase combination (LC) and ionosphere-free pseudo range combination (PC) type. The typical value of sigma on LC type is less than 1 cm which suggested by GIPSY/OASIS GD2P_PPP official manual. According the processing result from 1993 to May 2017, there are more than 95% data are well solved. The sigma on X, Y, and Z components are 1.9 mm, 1.7 mm, and 1.5 mm, respectively. This result suggests us the constraint we use in GIPSY data processing should be reasonable.

Also, the sigma value helps us to do station quality control. The station LUSN which is located at the central TW shows 0% data can be solved. In the other words, the LUSN station should improve the surrounding environment situation or migrate the location. About the coseismic deformation of 2016 Feb. 6 Meinong earthquake, the result shows similar pattern with GAMIT/GLOBK. It realizes GIPSY would be dependable in this case.

Keywords: GPS, GIPSY

NOTES

Ultra-low-frequency geomagnetic anomaly associated with Taiwan earthquakes

Fang-Ju Wu[1*], Guan-Hao,Peng[1] , Ting-Kuan Wen[1]

1. Seismological Center, Central Weather Bureau, Taiwan.
(fangju@scman.cwb.gov.tw)

The stress caused by the formation of regional geomagnetic field changes before the occurrence of many large earthquakes. Therefore, the Central Weather Bureau (CWB) has set up 12 stations to monitor variations of local geomagnetic total intensity field in Taiwan. In this study, we use ultra-low frequency analysis to find the association with earthquakes, which is using cross correlation values between the earthquake-related (0.01 – 0.1Hz) and relatively low (0.001 – 0.01Hz) frequency bands. When the correlation coefficient value getting low for several days that may be related to the earthquake precursors, and by showing the daily analysis of the station to facilitate the interpretation of ultra-low-frequency geomagnetic anomaly.

Keywords: ULF, geomagnetic

NOTES

Application of GNSS Observational Networks about Temporal and Spatial Monitoring in Ionospheric Earthquake Precursors

Shih-Han Chien[1*]

1. Seismological Center, Central Weather Bureau, Taiwan.
(justin510199@scman.cwb.gov.tw)

Numerous studies indicate the possibility of a relationship between ionosphere total electron content (TEC) short-term disturbances and large earthquakes. Indeed, the phenomena of ionospheric anomaly variation has attracted the attention of scientists for many years. Moreover, TEC variation seems to be one possible method to identify earthquake precursors. In previous TEC measurement, the ground-based dual-frequency Global Positioning System (GPS) technique is the principal means of remote sensing the TEC over dry land. New TEC calculation technique produced by Central Weather Bureau provides better spatial distribution as the result for adding Beidou satellite system. The United States GPS and Beidou satellite system from China are both including in Global Navigation Satellite System (GNSS) respectively. In our study, we demonstrate temporal and spatial distribution of TEC in near Taiwan area with sampling time 1 hour. Besides, monitoring anomaly variation in TEC is our routine work for every single day. In addition to operative monitoring service. We using Global Ionosphere Map (GIM) to analyze the relationship between TEC anomaly variation and earthquakes happened in Taiwan during 2000-2016, threshold is set by earthquake magnitude over 6.0, depth under 30 kilometers. Also, time interval with 1-10 days before earthquake happened all without geomagnetic storm. In the end, totally 15 earthquake cases are selected. The results present different conditions of 1-3 days TEC anomaly disturbance before earthquake. In spite that not all of large earthquakes discover the ionosperic precursors. Moreover, geophysical mechanism how earthquakes generated electron density has not been validated yet. But we still believe the above-mentioned studies and routine monitoring may provide some new and beneficial insights for the future study of ionospheric earthquake precursors.

Keywords: GNSS, TEC anomaly, Earthquake Precursors

NOTES

Spatial and temporal characteristics of the microseismicity preceding the 2016 M_L 6.6 Meinong earthquake in southern Taiwan

Hsin-Chieh Pu[1*]

1 .Seismological Center, Central Weather Bureau, Taiwan
(pu@scman.cwb.gov.tw)

Before the M_L 6.6 Meinong earthquake in 2016, a number of specific seismic behaviors were extracted from a comprehensive earthquake catalog provided by the Central Weather Bureau Seismological Network 24 bits. These specific seismic behaviors are considered to be intermediate-term quiescence, foreshocks, and short-term quiescence. In practice, these behaviors are thought to be the seismic indicators of an earthquake precursor, and their spatiotemporal characteristics may be associated with some of the source parameters of the following main shock. Hence, a series of detailed examinations were carried out to derive the spatiotemporal characteristics of these meaningful seismic behaviors. First, the spatial range of the intermediate-term quiescence that occurred for ~ 96 days was identified within an area with a maximum radius of 11 km from the hypocenter of the Meinong earthquake. Second, a series of foreshocks was present for ~1 day, clustered at the southeastern end of the Meinong earthquake. Third, short-term quiescence was present for ~3 days and was pronounced after the foreshocks. In summary, the location of these meaningful seismic behaviors indicated the possible location of the following Meinong earthquake. The spatial range of the intermediate-term quiescence could be related to the magnitude of the following Meinong earthquake. During the period of this quiescence, the findings further indicate two areas with a local low seismicity rate which may be associated with the major asperities of the Meinong earthquake. Furthermore, a short-term warning for the Meinong earthquake could have been announced based on the occurrence of the short-term quiescence, which was pronounced after a series of clustered foreshocks. These valuable seismic behaviors were weak because the intermediate-term quiescence was characterized by microseismicity at the lower cut-off magnitude, between M_L 1.2 and 1.5, and the majority of the foreshocks were comprised of earthquakes with a magnitude lower than 1.8. Particularly, plausible intermediate-term quiescence of microseismicity also appeared before the Nantou earthquake on March 27, 2013. Therefore, intermediate-term quiescence, one of the precursory indicators, might be an anticipative phenomenon before a strong earthquake in Taiwan.

Keywords: seismic quiescence, foreshock, Meinong earthquake, earthquake precursor

NOTES

Shallow fault rupture triggered by main shock of the 2016 Meinong earthquake inferred by Multi-sight InSAR and GPS data

Ying-Hui Yang[1, 2*], Jyr-Ching Hu[2]

1. School of Civil Engineering and Architecture, Southwest Petroleum University, Chengdu, China..
2. Department of Geoscience, National Taiwan University, Taipei, Taiwan.
(xzhfhyyy@126.com)

Multi-sight and high spatial resolution Interferometric Synthetic Aperture Radar (InSAR) data and high-accuracy GPS data are used to characterize the fault geometry and slip distribution of the 2016 Mw 6.5 Meinong earthquake in Taiwan. The main fault ruptured at depth of 10-24 km and was dominated by the right-strike slip with an average magnitude of ~0.5 m in the high-slip patches. But it is found that the single main fault failed to provide a good fit to coseismic deformation observed from multi-sight InSAR and GPS measurements simultaneously. Here, the shallow Lungchuan fault dipping to west with varying dip angles along the down-dip direction is found to have been triggered during the Meinong earthquake, which contributed major deformation between Lungchuan and Guanmiao faults. Another shallow Guanmiao fault dipping to west with a uniform dip angle of 23.7º also has been triggered in the Meinong event, which controlled the localized surface deformation in the Guanmiao zone. The Coulomb failure stress (CFS) changes on shallow listric Lungchuan fault and planar Guanmiao fault derived from the main fault slip are ~0.5 bar and ~0.1 bar, which are both sufficient to trigger the rupture if these faults are critically stressed and close to failure. The seismic moment of our preferred faulting model is 7.78×10^{18} Nm, equaling to Mw 6.7 event, and it is greater than 4.26×10^{18} Nm (Mw 6.4) of the CWB solution, which should be resulted from the seismic moment of the two found shallow faults. The result of this study suggests that a moderate earthquake has the potential to trigger the fault rupture at the shallow crust, and then results in severe surface motion and seismic hazard.

Keywords: InSAR, Triggered shallow fault rupture, Coulomb stress change, Meinong earthquake.

NOTES

Characterizing the deformation pattern of Mass Rapid Transportation in Taipei basin by SAR interferometry

Pei-Chin Wu [1*]

1. Department of Geosciences, National Taiwan University, Taipei, Taiwan.
(r03224206@ntu.edu.tw)

It is well known that a great amount wells in the Taipei Basin are used for water supply. Yet, the overuse of ground water leads to land subsidence up to 5 cm annually in Taipei basin. Although the government had begun to limit groundwater pumping since 1968, the groundwater in the Taipei Basin demonstrated temporary fluctuation. This phenomenon is induced by water pumping for large deep excavation site or engineering usage. In this study, 37 high-resolution X-band COSMO-SkyMed radar images from May 2011 to April 2015 is used to characterize deformation pattern in the period of construction of Mass Rapid Transportation (MRT). 30 wells and 320 benchmarks of precise leveling in Taipei basin is also used to study the correlation of surface deformation and change of ground water table. The storability is roughly constant across most of the aquifer with values between 0.8 x 10-4 and 1.3 x 10-3.

Moreover, the high water pumping in two major aquifers, Jignme and Wuku Foramtions, before the underground construction for MRT has led to the infliction of surface deformation. No time delay is observed for surface deformation during the water pumping. It is implied that the poro-elastic effect dominates in major aquifers in Taipei basin.

Keywords: PS-InSAR, Groundwater, Surface deformation.

NOTES

Citizen Seismology for Earthquake Early Warning System

Da-Yi Chen[1*]

1. Seismological Center, Central Weather Bureau, Taiwan.
(dayi@scman.cwb.gov.tw)

Internet of things (IOT) is the concept of every object connecting with each other via network. Recently the communication and electronics technology have been improved to make this ideas come true. Makers can easily find cheap sensors and developing board to construct any system. Here, in order to educate people the concept of the earthquake early warning (EEW) and make them contribute to this field, an EEW system was established by the IOT technology. In the beginning, this study can be tested in the school. Students can make their own seismic network and data processing center by themselves. The real-time data can be integrated in a data processing center of each school. We can further integrate all data processing centers to make a larger seismic network for monitoring earthquakes and implementing EEW system.

By using a Wi-Fi available developing board, named LinkIt™ Smart 7688, to connect three-component accelerometer, a real-time seismic sensor was constructed. The developing board has Linux operation system inside. Real-time data can be received by the developing board. Then, the data can be transmitted to another computer for data processing. In this study, we tried to write a program to receive data in the data processing center and setup the Earthworm software, initially developed by the United States Geological Survey, for integrating real-time data from the seismic sensors. Finally, the data processing center can not only display, archiving, exchanging, and processing data, but also implement the Earthworm based EEW modules, which was developed by the Central Weather Bureau (Chen et al., 2015). An IOT based EEW system have been developed and tested.

NOTES

A Study of Site Effect on Station Corrections of Magnitude and Measurement of the Spectral Decay Parameter Kappa Using Borehole Seismic Array Data

Tz-Shin Lai[1, 2], Yih-Min Wu[2], Wei-An Chao[3]

[1]Seismological Center, Central Weather Bureau
[2]Department of Geosciences, National Taiwan University
[3]Department of Civil Engineering, National Chiao Tung University
(heidi@scman.cwb.gov.tw)

Seismic stations including the Broadband Array in Taiwan for Seismology (BATS) were incorporated within the Central Weather Bureau Seismic Network (CWBSN) since 2012. However, site effects of seismic stations have not been applied for M_{L} determination that it may affect the magnitude estimation. Moreover, the appearance of relatively low seismicity is observed in 2012 from monthly event counts for M_{L} >2.0. Thus, we would like to examine whether there is a relationship between the updated seismic network and low seismicity or not. In this study, we first collect the earthquake catalog data during the period from 1994/01/01 to 2014/12/31 to calculate the station correction in order to reduce site effect in estimating magnitude. There is a strong correlation between station correction and near-surface geology beneath the station. Stations located on soil sites have high amplifications with negative station corrections. In contrast, stations located on hard rock sites have low amplifications with positive station corrections. After applied the station corrections to revise M_{L} estimation, the monthly event-occurrence rates return inside the range of one standard deviation in 2012 and revealed no low or high anomaly. Therefore, the reason low seismicity in 2012 is that new seismic stations which are installed on rock sites lead to underestimate of the magnitude determination. Next, we investigate the spectral decay parameter kappa (κ) to get more information for site effects of seismic stations. We used 133 earthquakes recorded by 30 borehole seismic array deployed by Central Weather Bureau (CWB) to estimate the κ value. Each vertical array includes two force balance accelerometers at the surface and the borehole. Based on the regression analysis between κ value and hypocentral distance for each surface-borehole station pairs, most of resulting κ_0 derived from surface stations are higher than results of borehole stations. These valuable dataset of κ_0 values offer an excellent opportunity for us to evaluate the quality factor (Qs) at shallow depths. In comparison with a study of site corrections, these higher κ_0 values associated with negative station corrections can correspond to

effect of soil conditions. In order to determine the linear relationship between station corrections and κ_0 values, we find the co-site stations of TSMIP and CWBSN to estimate κ_0 and the regression line. In this study, the station corrections of magnitude and κ_0 values both can investigate the site effects beneath the stations. Furthermore, the regression line of these two can be the information for the estimation of earthquake magnitude including borehole stations in the future.

Keywords: site effects、station corrections、kappa、borehole seismic array、local magnitude

NOTES

Developing a Near Real-time Automatic System for Rupture Inversions of Moderate and Large Earthquakes

Yi-Ching Lo[1*], Li Zhao[2], and Shu-Huei Hung[1]

1. Department of Geosciences, National Taiwan University.
2. Institute of Earth Sciences, Academia Sinica.
(jinglo@scman.cwb.gov.tw)

Moderate earthquakes (M_W6 or above) occur in Taiwan frequently and can cause significant damages to the society. As a result, developing capabilities for earthquake early warning and hazard mitigation has always been an important task for the Earth science community. After the occurrence of earthquakes, rapid report of relevant source information including the event location, magnitude, and the focal mechanism, is not only necessary for seismotectonic studies but also crucial for disaster relief operations as well as for the demands of the general public for information dissemination.

We report the development of a computational platform in the Central Weather Bureau (CWB) of Taiwan for near real-time automatic inversions of earthquake source parameters for early warning purpose. In our source inversion system, focal mechanisms are automatically obtained in real-time for all felt earthquakes in Taiwan. For relatively large earthquakes, the increased complexities in both space and time of the faulting processes demands that more detailed characteristics of the sources be considered to characterize their spatial-temporal variations in order to capture the directivity effects on the radiation of seismic waves. Therefore, for moderate and large earthquakes, our system involves two types additional operations: (1) Slip-distribution inversions of global earthquakes of large magnitude (M_W6.7 and above) using teleseismic records from global seismic network; and (2) a regional component for inversions of moderate and large earthquakes (M_W6.0 and above) in and around Taiwan using regional networks (such as the Broandband Array in Taiwan for Seismology, BATS).

Keywords: Finite-source slip distribution, source inversion, Rupture process, seismic hazard

NOTES